AD-A197 647

THEORETICAL STUDY OF THE RADIATIVE AND KINETIC PROPERTIES OF SELECTED METAL OXIDES AND AIR MOLECULES

H. H. Michels
United Technologies Research Center
400 Main Street
East Hartford, CT 06108

2 March 1988

Technical Report

CONTRACT No. DNA 001-85-C-0120

DTIC
ELECTE
JUL 08 1988
D

Prepared for
  Director
  DEFENSE NUCLEAR AGENCY
  Washington, DC 20305-1000

Destroy this report when it is no longer needed. Do not return
to sender.

REPORT DOCUMENTATION PAGE

1a. REPORT SECURITY CLASSIFICATION	1b. RESTRICTIVE MARKINGS
UNCLASSIFIED	

2a. SECURITY CLASSIFICATION AUTHORITY	3. DISTRIBUTION/AVAILABILITY OF REPORT
N/A since Unclassified	Approved for public release; distribution is unlimited.
2b. DECLASSIFICATION/DOWNGRADING SCHEDULE	
N/A since Unclassified	

4. PERFORMING ORGANIZATION REPORT NUMBER(S)	5. MONITORING ORGANIZATION REPORT NUMBER(S)
UTRC-927149	DNA-TR-88-12

6a. NAME OF PERFORMING ORGANIZATION	6b. OFFICE SYMBOL (If applicable)	7a. NAME OF MONITORING ORGANIZATION
United Technologies Research Center		Director Defense Nuclear Agency

6c. ADDRESS (City, State and ZIP Code)	7b. ADDRESS (City, State and ZIP Code)
400 Main Street East Hartford, CT 06108	Washington, DC 20305-1000

8a. NAME OF FUNDING/SPONSORING ORGANIZATION	8b. OFFICE SYMBOL (If applicable)	9. PROCUREMENT INSTRUMENT IDENTIFICATION NUMBER
	RAAE/Schwartz	DNA 001-85-C-0120

8c. ADDRESS (City, State and ZIP Code)	10. SOURCE OF FUNDING NOS.			
	PROGRAM ELEMENT NO.	PROJECT NO.	TASK NO.	WORK UNIT NO.
	62715H	Z	A	DH200772

11. TITLE (Include Security Classification) THEORETICAL STUDY OF THE RADIATIVE AND KINETIC PROPERTIES OF SELECTED METAL OXIDES AND AIR MOLECULES

12. PERSONAL AUTHOR(S)
Michels, H. H.

13a. TYPE OF REPORT	13b. TIME COVERED	14. DATE OF REPORT (Yr., Mo., Day)	15. PAGE COUNT
Technical	FROM 850502 TO 880302	880302	100

16. SUPPLEMENTARY NOTATION
This work was sponsored by the Defense Nuclear Agency under RDT&E RMC Code B322085760 Z A 00016 25904D.

17.	COSATI CODES		18. SUBJECT TERMS (Continue on reverse if necessary and identify by block number)
FIELD	GROUP	SUB. GR.	UO UO_2 UO_2^{++} Potential Energy Curves
4	1		UO^+ UO_2^+ TiO^+
11	6		

19. ABSTRACT (Continue on reverse if necessary and identify by block number)

A theoretical research program directed toward the study of the energetics and LWIR radiative properties of selected uranium/oxygen band systems has been undertaken. Included in this research program was the investigation of the strongest electronic and vibrational bands in the LWIR region for the species UO, UO^+, UO_2, UO_2^+, UO_2^{++} and TiO^+. The program for accomplishing this research effort was formulated into three separate tasks: a) adaption of our electronic structure codes to the DNA CRAY-I System, b) calculation of pertinent electronic wavefunctions and energies, as a function of internuclear separation and within a relativistic framework, for selected species of the uranium/oxygen system which may be important in the LWIR region, and c) calculation of electronic transition moments and transition probabilities between

20. DISTRIBUTION/AVAILABILITY OF ABSTRACT	21. ABSTRACT SECURITY CLASSIFICATION
UNCLASSIFIED/UNLIMITED ☐ SAME AS RPT ☒ DTIC USERS ☐	UNCLASSIFIED

22a. NAME OF RESPONSIBLE INDIVIDUAL	22b. TELEPHONE NUMBER (Include Area Code)	22c. OFFICE SYMBOL
Sandra E. Young	(202) 325-7042	DNA/CSTI

DD FORM 1473, 83 APR — EDITION OF 1 JAN 73 IS OBSOLETE

UNCLASSIFIED
SECURITY CLASSIFICATION OF THIS PAGE

19. ABSTRACT (Continued)

specific vibrational levels of the electronic states corresponding to the
strongest radiating band systems belonging to the uranium/oxygen and
titanium/oxygen systems and prediction of IR and possible optical oscillator
strengths.

The results obtained to date for the uranium/oxygen system indicate that
both UO^+ and UO_2^+ are very strong LWIR radiators in the 10-14 um region. In
addition, UO^+, which is a potential late time radiator, exhibits strong
visible bands and should be efficiently solar pumped. A careful evaluation of
the low-lying excited states of UO_2^+, particularly those charge transfer
states that arise by promotion of an electron from (mainly) ligand MO's to a
central uranium atom MO, indicates that such transitions lie well outside of
the region for efficient solar pumping of UO_2^+. However, the density of
electronic states for UO_2^+ lying below 8 eV is immense, and additional studies
are needed for this system.

A preliminary analysis of the titanium/oxygen system was also carried out
with emphasis on LWIR for TiO^+. An unexpected result of this work is our
conclusion that TiO^+ is a weak IR radiator with $f_{10} = 4.4 \times 10^{-6}$. This system
is thus down by perhaps a factor of 10 from the emission intensity of the UO^+
and UO_2^+ species. However, we find that TiO_2^+ may be an important radiator
and further characterization of this system is required.

Other studies within DNA chemistry requirements include a preliminary
analysis of dielectronic recombination of $e + U^{+q}$ and $e + UO^+$, which are
possible charge neutralization processes, and an analysis of the kinetics of
the $N + O_2$ and $O + N_2$ reactions in producing vibrationally hot NO molecules
radiating in the IR. Our analysis of dielectronic recombination indicates
that $e + U^{++}$ is not rate competitive with possible ion-neutral charge exchange
reactions but that $e + U^+$ may exhibit a large kinetic rate for neutraliza-
tion.

PREFACE

Accession For	
NTIS GRA&I	X
DTIC TAB	☐
Unannounced	☐
Justification	
By	
Distribution/	
Availability Codes	
	Avail and/or
Dist	Special
A-1	

DTIC
COPY
INSPECTED
6

CONVERSION TABLE

(Conversion factors for U. S. customary to
metric (SI) units of measurement)

To Convert From	To	Multiply By
angstrom	meters (m)	$1.000\ 000\ \text{X E} -10$
atmosphere (normal)	kilo pascal (kPa)	$1.013\ 25\ \text{X E} +2$
bar	kilo pascal (kPa)	$1.000\ 000\ \text{X E} +2$
barn	meter^2 (m^2)	$1.000\ 000\ \text{X E} -28$
British thermal unit		
(thermochemical)	joule (J)	$1.054\ 350\ \text{X E} +3$
cal (thermochemical)/cm^2	mega joule/m^2(MJ/m^2)	$4.184\ 000\ \text{X E} -2$
calorie (thermochemical)	joule (J)	$4.184\ 000$
calorie (thermochemical)/g	joule per kilogram (J/kg)	$4.184\ 000\ \text{X E} +3$
curie	giga becquerel (GBq)	$3.700\ 000\ \text{X E} +1$
degree Celsius	degree kelvin (K)	$t_K = t^°_C + 273.15$
degree (angle)	radian (rad)	$1.745\ 329\ \text{X E}-2$
degree Fahrenheit	degree kelvin (K)	$t_K = (t^°_F + 459.67)/1.8$
electron volt	joule (J)	$1.602\ 19\ \text{X E} -19$
erg	joule (J)	$1.000\ 000\ \text{X E} -7$
erg/second	watt (W)	$1.000\ 000\ \text{X E} -7$
foot	meter (m)	$3.048\ 000\ \text{X E} -1$
foot-pound-force	joule (J)	$1.355\ 818$
gallon (U.S. liquid)	meter^3 (m^3)	$3.785\ 412\ \text{X E} -3$
inch	meter (m)	$2.540\ 000\ \text{X E}-2$
jerk	joule (J)	$1.000\ 000\ \text{X E} +9$
joule/kilogram (J/kg)		
(radiation dose absorbed)	gray (Gy)	$1.000\ 000$
kilotons	terajoules	4.183
kip (1000 lbf)	newton (N)	$4.448\ 222\ \text{X E} +3$
kip/inch^2 (ksi)	kilo pascal (kPa)	$6.894\ 757\ \text{X E} +3$
ktap	newton-second/m^2 (N-s/m^2)	$1.000\ 000\ \text{X E} +2$
micron	meter (m)	$1.000\ 000\ \text{X E} -6$
mil	meter (m)	$2.540\ 000\ \text{X} -5$

CONVERSION TABLE (Concluded)

To Convert From	To	Multiply By
mile (international)	meter (m)	$1.609\ 344 \times E\ +3$
ounce	kilogram (kg)	$2.834\ 952 \times E\ -2$
pound-force (lbf avoirdupois)	newton (N)	$4.448\ 222$
pound-force inch	newton-meter (N·m)	$1.129\ 848 \times E\ -1$
pound-force/inch	newton/meter (N/m)	$1.751\ 268 \times E\ +2$
pound-force/foot^2	kilo pascal (kPa)	$4.788\ 026 \times E\ -2$
pound-force/inch^2 (psi)	kilo pascal (kPa)	$6.894\ 757$
pound-mass (lbm avoirdupois)	kilogram (kg)	$4.535\ 924 \times E\ -1$
pound-mass-foot^2 (moment of inertia)	kilogram-meter^2 (kg·m^2)	$4.214\ 011 \times E\ -2$
pound-mass/foot^3	kilogram-meter^3 (kg/m^3)	$1.601\ 846 \times E\ +1$
rad (radiation dose absorbed)	gray (Gy)	$1.000\ 000 \times E\ -2$
roentgen	coulomb/kilogram (C/kg)	$2.579\ 760 \times E\ -4$
shake	second (s)	$1.000\ 000 \times E\ -8$
slug	kilogram (kg)	$1.459\ 390 \times E\ +1$
torr (mm Hg, 0°C)	kilo pascal (kPa)	$1.333\ 22 \times E\ -1$

TABLE OF CONTENTS

LIST OF ILLUSTRATIONS

LIST OF TABLES

SECTION 1

INTRODUCTION

The release of certain chemical species into the upper atmosphere results in luminous clouds that display the resonance electronic-vibration-rotation spectra of the chemically reacting species. Such spectra are seen in rocket releases of chemicals for upper atmospheric studies, upon re-entry into the atmosphere of artificial satellites and missiles, and as a result of energy deposition in the atmosphere caused by nuclear weapons effects. Of particular interest in this connection is the observed spectra of certain metallic oxides. From band intensity distributions of the spectra, and knowledge of the f-values for electronic and vibrational transitions, the local conditions of the atmosphere can be determined (Reference 1). Such data are fundamental for the analysis of detection and discrimination problems.

Present theoretical efforts, which are directed toward a more complete and realistic analysis of the transport equations governing atmospheric relaxation and the propagation of artificial disturbances, require detailed information of thermal opacities and LWIR absorption in region of temperature and pressure where both atomic and molecular effects are important (References 2 and 3). Although various experimental techniques have been employed for both atomic and molecular systems, theoretical studies have been largely confined to an analysis of the properties (bound-bound, bound-free and free-free) of atomic systems (References 4 and 5). This has been due in large part to the unavailability of reliable wavefunctions for diatomic molecular systems, and particularly for excited states or states of open-shell structure. Only recently (References 6-8) have reliable procedures been prescribed for such systems which have resulted in the development of practical computational programs.

The application of these computational methods to studies of the electronic structure and radiation characteristics of metal oxides has been reported for several of the lighter systems (References 9-11). A preliminary study of the uranium/oxygen system has been reported by Michels (Reference 12) which identified a large number of low-lying molecular states for both the UO and UO^+ systems. Of particular interest was the discovery of two structures for UO^+ that resulted from two different spin-couplings of the uranium

valence electrons. These results suggested strong LWIR radiation in UO^+ arising from different electronic state transitions.

An inherent uncertainty in these preliminary calculations was present, owing to the neglect of relativistic effects that were much too difficult to include in molecular calculations at that period of time. The 7s valence electron of uranium, and its corresponding σ-bonding molecular orbital, are highly relativistic in nature which results in a contracted charge density relative to that which would occur in lighter molecular systems. The effect of this contraction on the relative positions of the low-lying electronic states of the uranium/oxygen system can now be calculated with some degree of confidence using newly developed relativistic computer codes.

Because of inherent difficulties in the experimental determination of the spectroscopy, transition probabilities and LWIR radiation for metal oxide systems and in light of the aforementioned recent progress in the calculation of relativistic electronic wavefunctions, especially for diatomic systems, a technical program for calculating these properties was undertaken for the Defense Nuclear Agency under Contracts DNA001-85-C-0120, DNA001-83-C-0044 and DNA001-82-C-0015. The emphasis in this work was on the ions of uranium and uranium oxide since these species have been determined to be important radiators in the LWIR region. These studies indicated that, in addition to UO^+ and UO_2^+, the doubly ionized species, U^{++}, UO^{++} and UO_2^{++}, should also be considered because of their role in charge neutralization processes and their potential as early-time radiators.

A summary of the results obtained to date for the uranium/oxygen system indicates that both UO^+ and UO_2^+ are very strong LWIR radiators in the 10-14 µm region. In addition, UO^+, which is a potential late time radiator exhibits strong visible bands and should be efficiently solar pumped. A careful evaluation of the low-lying excited states of UO_2^+, particularly those charge transfer states that arise by promotion of an electron from (mainly) ligand MO's to a central uranium atom MO, indicates that such transitions lie well outside of the region for efficient solar pumping. However, the density of electronic states for UO_2^+ lying below 8 eV is immense, and additional studies are needed for this system.

A preliminary analysis of the titanium/oxygen system was also carried out with emphasis on LWIR for TiO^+. An unexpected result of this work is our

conclusion that TiO^+ is a weak IR radiator with $f_{ij} = 4.4 \times 10^{-6}$. This system is thus down by perhaps a factor of 10 from the emission intensity of the UO^+ and UO_2^+ species. However, we find that TiO_2^+ may be an important radiator and further characterization of this system is required.

Other studies within DNA chemistry requirements include an analysis of dielectronic recombination of $e + U^+$ and $e + UO^+$ which, are possible charge neutralization processes, and an analysis of the kinetics of the $N + O_2$ and $O + N_2$ reactions in producing vibrationally hot NO molecules radiating in the IR. This report addresses theoretical studies in all of the areas described above.

The general composition of this report is as follows. In Section 2, we present a description of the mathematical methods which were employed in this research. Included in Section 2 are sub-sections which deal with the construction of electronic wavefunctions, the calculations of expectation properties, the evaluation of molecular transition probabilities, and the calculation of electronic wavefunctions using both the ab initio and density functional methods. This is followed by Section 3 which describes the inclusion of relativistic effects into the density functional (X_α) method. The calculated results and pertinent discussion are presented in Section 4. Recommendations are presented in Section 5.

SECTION 2

METHOD OF APPROACH - NONRELATIVISTIC METHODS

2.1 QUANTUM MECHANICAL CALCULATIONS.

Central to these theoretical studies are the actual quantum-mechanical calculations which must be carried out for the atomic and molecular species. In particular, the methodology for computing the minimum energy stable structures must be carefully analyzed. For added clarity, various aspects of these calculations are discussed below.

Much evidence on diatomic and polyatomic systems indicates the inadequacy of a minimum basis set for constructing quantitatively correct molecular wavefunctions (References 13 and 14). This means inner-shell and valence-shell orbitals of quantum numbers appropriate to the atoms (1s, 2s, 2p, for C, N, O; etc.). The main deficiency of the minimum basis set is its inability to properly describe polarization and the change of orbital shape for systems which exhibit large charge transfer effects. Values of the screening parameters for each orbital can either be set from atomic studies or optimized in the molecule; the latter approach is indicated for studies of higher precision. When high chemical accuracy is required, as for detailed studies of the ground or a particular excited state of a system, a more extended basis must be used. Double-zeta plus polarization functions or optimized MO's are usually required as a minimum representation for reliable calculated results of chemical accuracy.

The chosen basis sets give good results only when used in a maximally flexible manner. This implies the construction of perturbation expansions or the use of CI wavefunctions with all kinds of possible orbital occupancies, so that the correlation of electrons into overall states can adjust to an optimum form at each geometrical conformation and for each state. Except when well-defined pairings exist, as for closed shell and exchange dominated systems, a single-configuration study (even of Hartree-Fock quality) will be inadequate.

Proper electronic states for systems composed of light atoms should possess definite eigenvalues of the spin operator S^2 as well as an appropriate geometrical symmetry. The geometrical symmetry can be controlled by the assignment of orbitals to each configuration, but the spin state must be

4

obtained by a constructive or projective technique. Formulas have been developed (Reference 15) for projected construction of spin states from orthogonal orbitals, and programs implementing these formulas have been in routine use at UTRC for several years. One of the least widely appreciated aspects of the spin-projection problem is that the same set of occupied spatial orbitals can sometimes be coupled to give more than one overall state of a given spin quantum number. It is necessary to include in calculations all such spin couplings, as the optimum coupling will continuously change with changes in the molecular conformation. This is especially important in describing degenerate or near-degenerate excited electronic states.

In the sections below, we describe the several mathematical approaches that are applicable to calculation of the potential energy surfaces for chemically reacting systems and to the subsequent calculation of transition probabilities and f-numbers. Since several different approaches are indicated, we describe their expected regions of applicability.

2.1.1 Method of Ab Initio Calculation.

2.1.1.1 Born-Oppenheimer Separation.

For a system of n electrons and N nuclei, and considering only electro-static interactions between the particles, we have for the total Hamiltonian

$$\mathscr{H} = \mathscr{H}_{el} - \sum \frac{\hbar^2}{2m_\alpha} \nabla_\alpha^2 + \frac{\hbar^2}{2M_T} \left[\sum_{\substack{\beta=1 \\ \alpha \neq \beta}}^{N} \sum_{\alpha=1}^{N} \nabla_\alpha \cdot \nabla_\beta \right.$$
$$\left. + 2 \sum_{\alpha=1}^{N} \sum_{i=1}^{n} \nabla_\alpha \cdot \nabla_i + \sum_{i=1}^{n} \sum_{\substack{j=1 \\ i \neq j}}^{n} \nabla_i \cdot \nabla_j \right] \tag{1}$$

where

$$\mathscr{H}_{el} = - \frac{\hbar^2}{2m_e} \sum_{i=1}^{n} \nabla_i^2 + V^{el}(\underline{r}_n, \underline{R}_N) \tag{2}$$

and where m_e, m_α, M_T, are the masses of the electron, atom α and combined system mass, respectively. Now since the ratios m_e/m_α and m_e/M_T are both small, $(2 \cdot 10^{-6} - 5 \cdot 10^{-4})$ we can effect a separation of the electronic and

5

nuclear coordinates treating the total wavefunction as a product of a nuclear and an electronic part. We have

$$\psi(\underset{\sim}{r}_n, \underset{\sim}{R}_N) = \sum_k \chi_k(\underset{\sim}{R}_N) \psi_k(\underset{\sim}{r}_n, \underset{\sim}{R}_N) \tag{3}$$

where $\psi_k(\underset{\sim}{r}_n, \underset{\sim}{R}_N)$ is an electronic wavefunction parametric in the nuclear coordinates as given in Equation (3) and $\chi_k(\underset{\sim}{R}_N)$ are nuclear motion wavefunctions which satisfy (neglecting terms of the order of m_e/M_α)

$$\left[-\sum_{\alpha=1}^{N} \frac{\hbar^2}{2m_\alpha} \nabla_\alpha^2 + \frac{\hbar^2}{2M_T} \sum_{\substack{\alpha=1 \\ \alpha \neq \beta}}^{N} \sum_{\beta=1}^{N} \nabla_\alpha \cdot \nabla_\beta + V^{el}(\underset{\sim}{r}_n, \underset{\sim}{R}_N) \right] \chi_k = i\hbar \frac{\partial \chi_k}{\partial t} \tag{4}$$

The cross term in $\nabla_\alpha \cdot \nabla_\beta$ can be eliminated by a proper change of variables and Equation (4) then reduces to a 3N-3 dimensional Schrödinger equation.

For most systems, where the velocity of motion of the nuclei is slow relative to the electron velocity, this decoupling of electron and nuclear motion is valid and is referred to as the adiabatic approximation. Equation (3) thus defines an electronic eigenstate $\psi_k(\underset{\sim}{r}_n, \underset{\sim}{R}_N)$, parametric in the nuclear coordinates, and a corresponding eigenvalue $E_k(\underset{\sim}{R}_N)$ which is taken to represent the potential energy curve or surface corresponding to state k.

2.1.1.2 Variational Methods. By an ab initio method is meant one that starts from a zero-order Hamiltonian which is exact except for relativistic and magnetic effects, and which involves the evaluation of electronic energies and other relevant quantities for wavefunctions which are properly antisymmetrized in the coordinates of all the electrons. For a system containing n electrons and M nuclei, the zero-order Hamiltonian depends parametrically on the nuclear positions and is of the form

$$\mathcal{H} = -\frac{1}{2} \sum_{i=1}^{n} \nabla_i^2 - \sum_{i=1}^{n} \sum_{j=1}^{M} \frac{Z_j}{|\vec{r}_i - \vec{R}_j|} + \sum_{1 \leq i < j}^{M} \frac{Z_i Z_j}{|\vec{R}_i - \vec{R}_j|} + \sum_{1 \leq i < j} \frac{1}{|\vec{r}_i - \vec{r}_j|} \tag{5}$$

where Z_i and $\vec{R}_i$ are the charge and position of nucleus i, $\vec{r}_j$ is the position of electron j, and ∇_j^2 is the Laplacian operator for electron j. All quantities are in atomic units, i.e. lengths in bohrs, energies in hartrees

6

(1 hartree = 2 Rydbergs). The many-electron wavefunction consists of one, or a linear combination, $\psi = \sum_\mu c_\mu \psi_\mu$, of terms of the form

$$\Psi_\mu(R) = \mathcal{A}\,\mathcal{O}_s \prod_{i=1}^{n} \Psi_{\mu i}(\underline{r}_i, R)\,\theta_M \tag{6}$$

where each $\phi_{\mu i}$ is a spatial orbital, $\mathcal{A}$ is the antisymmetrizing operator, $\mathcal{O}_s$ is the spin-projection operator for spin quantum number S, and $\theta_{\mu M}$ is a product of α and β one-electron spin functions of magnetic quantum number M_S. No requirement is imposed as to the double occupancy of the spatial orbital, so linear combinations of the form given by Equation (6) can describe a completely general wavefunction. The spatial orbitals $\phi_{\mu i}$ may be whatever basis orbitals have been introduced, arbitrary linear combinations thereof, or specific linear combinations determined pursuant to the particular calculational method in use.

The spatial orbitals $\phi_{\mu i}$, the spin functions $\theta_{\mu m_s}$, and the coefficients of different ψ_μ, if a linear combination of ψ_μ is used, may be explicitly determined by invoking the variational principle. Various specific methods are described below for determining wavefunctions. However, we should first observe that the adequacy of an ab initio calculation, or for that matter any energy calculation, will depend crucially upon the extent to which the wavefunction can be qualitatively appropriate. Some of the considerations surrounding the choice of a wavefunction are the following:

(i) necessity that the wavefunction possess sufficient flexibility to be able to describe dissociation to the correct atomic and molecular fragments as various internuclear separations are increased;

(ii) maintenance of equivalent quality of calculation for nuclear geometries differing in the nature or number of chemical bonds;

(iii) ability to describe degenerate or near-degenerate electronic states when they are pertinent;

(iv) ability to describe different electronic states to equivalent accuracy when their interrelation (e.g., crossing) is relevant, in particular, ability to describe ionic-valence state mixing;

(v) ability to represent changes in the coupling of electron spins as bonds are broken or reformed.

The foregoing considerations indicate that it will often be necessary to consider wavefunctions with more than a minimum number of singly-occupied spatial orbitals, and that there will be many potential curves or surfaces for which a wavefunction consisting of a single ψ_μ cannot suffice. It will then be necessary to allow mixing of ψ_μ with different degrees of orbital spatial occupancy so as to obtain smooth transitions from the occupancies characteristic of separated atoms or molecules (or ions) to those characteristic of a compound system or a different fragmentation.

Another implication of the considerations surrounding the choice of a wavefunction is related to the treatment of electron spin. Not only is it necessary to require that the wavefunction be an eigenfunction of S^2 and S_z but it is also necessary to take account of the fact that under many conditions, there will be more than one spin eigenfunction of given S and M_s. The different spin eigenfunctions correspond to different couplings among the individual spins. Since reactive processes involve the breaking and forming of electron-pair bonds, they must necessarily be accompanied by reorganizations of the spin coupling. A failure to take account of this will lead to qualitatively inappropriate wavefunctions.

In Hartree-Fock calculations $\psi(R)$ is restricted to a single ψ_μ which is assumed to consist as nearly as possible of doubly-occupied orbitals. The orbitals $\phi_{\mu i}$ are then selected to be the linear combinations of basis orbitals best satisfying the variational principle. Writing $\phi_{\mu i} = \sum_\nu a_{\nu i} \chi_\nu$, the $a_{\nu i}$ are determined by solving the matrix Hartree-Fock equations

$$\sum_\nu F_{\lambda\nu} a_{\nu i} = \epsilon_i \sum_\nu S_{\lambda\nu} a_{\nu i} \quad \text{(each } \lambda) \tag{7}$$

where ϵ_i is the orbital energy of $\phi_{\mu i}$.

The Fock operator $F_{\lambda\nu}$ has been thoroughly discussed in the literature (Reference 16) and depends upon one- and two-electron molecular integrals and upon the $a_{\nu i}$. This makes Equation (7) nonlinear and it is therefore solved iteratively. UTRC has developed programs for solving Equation (7) for both closed and open-shell systems, using basis sets consisting of Slater-type atomic orbitals. Examples of their use are in the literature (Reference 7).

In configuration interaction calculations, the overall wavefunction has more than one term, ψ_μ, and the c_μ are determined by invoking the variational principle to obtain the secular equation

$$\sum_\nu (H_{\mu\nu} - w S_{\mu\nu}) c_\nu = 0 \qquad (\text{each } \mu)\qquad(8)$$

where

$$H_{\mu\nu} = \int \Psi_\mu^*(R) \mathcal{H}(R) \Psi_\nu(R)\, d\tau$$

$$S_{\mu\nu} = \int \Psi_\mu^*(R) \Psi_\nu(R)\, d\tau \qquad(9)$$

Equation (8) is solved by matrix diagonalization using either a modified Givens method (Reference 17) or a method due to Shavitt (Reference 18) or Raffenetti (Reference 19).

The matrix elements $H_{\mu\nu}$ and $S_{\mu\nu}$ may be reduced by appropriate operator algebra to the forms

$$H_{\mu\nu} = \sum_P \epsilon_P \left\langle \theta_M \middle| \mathcal{O}_S P \middle| \theta_M \right\rangle \left\langle \prod_{i=1}^n \Psi_{\mu i}(r_i, R) \middle| \mathcal{H}(R) P \middle| \prod_{i=1}^n \Psi_{\nu i}(r_i, R) \right\rangle \qquad(10)$$

$$S_{\mu\nu} = \sum_P \epsilon_P \left\langle \theta_M \middle| \mathcal{O}_S P \middle| \theta_M \right\rangle \left\langle \prod_{i=1}^n \Psi_{\mu i}(r_i, R) \middle| P \middle| \prod_{i=1}^n \Psi_{\nu i}(r_i, R) \right\rangle \qquad(11)$$

where P is a permutation and ϵ_P its parity. The sum is over all permutations. $\langle \theta_M | \mathcal{O}_S P | \theta_M \rangle$ is a "Sanibel coefficient" and the remaining factors are spatial integrals which can be factored into one- and two-electron integrals. If the $\phi_{\mu i}$ are orthonormal, Equations (10) and (11) become more tractable and the $H_{\mu\nu}$ and $S_{\mu\nu}$ may be evaluated by explicit methods given in the literature (Reference 15). Computer programs have been developed for carrying out this procedure, and they have been used for problems containing up to 106 total electrons, 10 unpaired electrons, and several thousand configurations.

9

The CI studies described above can be carried out for any orthonormal set of $\phi_{\mu i}$ for which the molecular integrals can be calculated. Programs developed by UTRC make specific provision for the choice of the $\phi_{\mu i}$ as Slater-type atomic orbitals, as Gaussian-type orbitals, as symmetry molecular orbitals, as Hartree-Fock orbitals, or as more arbitrary combinations of atomic orbitals.

The one- and two-electron integrals needed for the above described method of calculation are evaluated for STO's by methods developed by this Center (Reference 20). For Gaussian orbitals, either the Carnegie-Mellon integral package (Reference 21) or the integral routines incorporated in the GAMESS program (Reference 22) can be employed. All needed computer programs have been fully tested at UTRC.

2.1.1.3 <u>Configuration Selection</u>. Using a double-zeta plus polarization basis set of one-electron functions, a typical system can have of the order of 10^5 configurations in full CI (that resulting from all possible orbital occupancies). It is therefore essential to identify and use the configurations describing the significant part of the wavefunction. There are several ways to accomplish this objective. First, one may screen atomic-orbital occupancies to eliminate configurations with excessive formal charge. Alternatively, in a molecular-orbital framework, one may eliminate configurations with excessive numbers of anti-bonding orbitals. A third possibility is to carry out an initial screening of configurations, rejecting those whose diagonal energies and interaction matrix elements do not satisfy energy significance criteria.

Another common method of classifying configurations is to examine the total number of orbitals in the wavefunction that differ from the SCF reference wavefunction. We write the CI wavefunction as

$$\psi_{CI} = C_o \psi_o + \sum_i C_i \phi_i^S + \sum_j C_j \phi_j^D + \ldots \tag{12}$$

where a single excitation function, ϕ_i^S, differs from the SCF reference ψ_o by one orbital and the double excitation function ϕ_j^D by two, and so on. The CI coefficients, C_i, are then determined variationally to yield the lowest possible total energy. In the limit of a complete basis set ($N \to \infty$), and where all possible substitutions are included in ψ_{CI}, the variational energy approaches the correct nonrelativistic Born-Oppenheimer result. Errors arise

10

from a truncation of the functions used to determine the SCF reference wave-function and from the truncation of the excitation functions series in ψ_{CI}. The reference wavefunction ψ_o will typically be the same for a CI or Many Body Perturbation Theory (MBPT) calculation; however, for a molecule even as small as water, ψ_{CI} becomes a function of a very large number of basis functions. Because of this, one must truncate the expansion and eliminate unimportant configurations. In general one can show that

$$\langle \psi_o | \mathcal{H} | \phi^T \rangle = \langle \psi_o | \mathcal{H} | \phi^Q \rangle = 0 \tag{13}$$

In words, the matrix elements between the reference wavefunction and triple and quadruple excitations is zero. Thus to first order, only single and double excitations contribute. Because of this, many CI calculations attempt to include all single and double excitations in the expressions for ψ_{CI}. To go beyond this, generally more than one reference wavefunction is used. Programs to handle configurations on all the above criteria are available at UTRC.

Other, potentially more elegant methods of configuration choice involve formal approaches based on natural-orbital (Reference 23) or multiconfigura-tion SCF (Reference 24) concepts. To implement the natural-orbital approach, an initial limited-CI wavefunction is transformed to natural-orbital form, and the resulting natural orbitals are used to form a new CI. The desired result is a concentration of the bulk of the CI wavefunction into a smaller number of significant terms. The multiconfiguration SCF approach is more cumbersome, but in principle more effective. It yields the optimum orbital choice for a preselected set of configurations. This approach works well when a small number of dominant configurations can be readily identified. The method is described briefly below.

2.1.1.4 <u>Multiconfiguration - Self Consistent Field Method (MC-SCF)</u>. The Hartree-Fock self consistent field method has been proven to be a powerful tool for the calculation and understanding of many ground state properties of molecules in the vicinity of their equilibrium structure. However, in most cases the one determinant Hartree-Fock approximation is not adequate to properly describe the dissociation of molecular bonds. Also, many excited states cannot be represented by a single configuration wave function. In order to calculate properties of such states or to investigate the formation

11

of molecular bonds one often needs multiconfiguration wave functions for which both the linear coefficients, C_i of the configuration expansion

$$\Psi = \sum_i C_i \psi_i \qquad (14)$$

as well as the set of orthonormal molecular orbitals $\{\phi_j\}$, from which the configurations ψ_i are constructed, are optimized according to the variational principle. As is well known, this "MC-SCF" problem presents many more difficulties than the simple one determinant Hartree-Fock case and much work has been devoted to obtaining convergent solutions during the last decade.

The difficulties mainly arise from the fact that for general MC-SCF wave functions the energy is not invariant with respect to rotations between occupied orbitals. Hence, instead of a relatively simple pseudo-eigenvalue equation in the one determinant case, the set of coupled Fock equations

$$\sum_j F_{ij} |\phi_j\rangle = \sum_j \varepsilon_{ij} |\phi_j\rangle, \qquad (15)$$

with the hermiticity conditions

$$\varepsilon_{ij} = \varepsilon_{ji}^* \qquad (16)$$

has to be solved. ε_{ij} are Lagrange multipliers which account for the orthonormality constraints imposed on the orbitals. The Fock operators F_{ij} depend on the orbitals $\{\phi_i\}$ and the set of CI coefficients $\{C_i\}$. In analogy to the one determinant case many attempts have been made to solve these equations iteratively by keeping the Fock operators fixed in each iteraction step. Then the Lagrange multipliers can be expressed by coupling operators constructed such that the Fock equations are transformed into pseudo-eigenvalue equations yielding the improved orbitals. These are used in a second step to determine new CI coefficients by diagonalizing the CI matrix $\langle \psi_i | \mathcal{H} | \psi_j \rangle$. The convergence of these algorithms, however, has often been found to be poor.

A second group of MC-SCF methods is based on the generalized Brillouin theorem. In these methods, the orbital changes are derived from the coefficients of a CI expansion consisting of the MC-SCF wavefunction and all one-electron singly excited configurations. A computer program (ALIS) implementing this method has been developed by Ruedenberg, et al (Reference 25). A somewhat more elegant program (GAMESS) which utilizes analytical gradients is also available (Reference 22). More recently, various methods have been

proposed which are based on direct minimization of the energy, avoiding the
Fock operators altogether. Such methods are now being studied in our labora-
tory and will be incorporated into our existing computer programs if they
prove to be highly efficient.

2.1.1.5 <u>Many-Body Perturbation Theory (MBPT)</u>. In MBPT we again begin with
the SCF wavefunction (ψ_o) as our reference and attempt to account for E_c,
the correlation energy. The concept of excitation functions described in the
above section on CI calculations carries over to MBPT calculations. In MBPT
one can write the wavefunction, ψ_p, as

$$\psi_p = e^T |\phi_o\rangle \qquad (17)$$

where T is an excitation operator defined as

$$T = T_S + T_D + T_T + T_Q \cdots \qquad (18)$$

where S, D, T, and Q refer to single, double, triple, and quadruple substi-
tutions respectively. One can write T_n, in general, where n refers to the
number of excitations as

$$T_n = \frac{1}{n!} \sum_{\substack{ijk\ldots \\ abc\ldots}} t_{ijk\ldots}^{abc\ldots} \chi_a^+ \chi_b^+ \chi_c^+ \cdots \chi_i \chi_j \chi_k \qquad (19)$$

where a,b,c,... are excited orbitals and i,j,k,... are orbitals occupied in
ϕ_o. The total energy is now given by

$$E_{MBPT} = \langle \phi_o | \mathcal{H} e^T | \phi_o \rangle \qquad (20)$$

To evaluate E_{MBPT}, the $t_{i\ldots}^{a\ldots}$ from above must be determined. An equivalent
expression that makes the perturbation expansion clearer is

$$E_{MBPT} = \sum_{k=0}^{\infty} \langle \phi_o | \mathcal{H}[(E_o - \mathcal{H}_o)^{-1} \mathcal{H}]^k | \phi_o \rangle \qquad (21)$$

where the sum is over only so called linked diagrams, $\mathcal{H}_o$ has eigenfunctions
ϕ_o, and the expansion is of orders in the perturbation, $V = (\mathcal{H} - \mathcal{H}_o)$. The
k = 0 term gives the reference energy and for k > 0 correlation corrections

are included. In practice the MBPT total energy is calculated by truncating the T operator expansion and projecting $\mathcal{H}e^{T_n}|\phi_o\rangle$ onto the appropriate n-space. This leads to a set of nonlinear coupled equations for the $t^{a\ldots}_{i\ldots}$ coefficients which correspond to the CI expansion coefficients. The equations are solved iteratively and E_{MBPT} evaluated. In practice T_4 is an upper limit that corresponds to quadruple substitutions. The series is an oscillatory convergent sum, which in practice has proven to be at least as accurate as E_{CI} with single and double excitations included.

The best possible method to use would be a full CI (all possible configurations) with a complete basis set. However, since the number of configurations is proportional to $\langle n|^{\ell}$, where n is the number of basis functions and ℓ is the level of excitation, it is usually prohibitive to even include all single and double excitations. This truncation causes the loss of size consistency, which implies that the energy calculated for A and B as a molecular system, but far apart, is the sum of the energy calculated for A and B separately. In a size extensive calculation the energy is proportional to the size of the system. These properties are very important if one wishes to compute correct relative energies on a potential energy surface, a necessary criteria for defining the reactive charge transfer pathways of interest in this research program. MBPT, on the other hand, is guaranteed to have the correct size-dependence because the expansions contain only the so-called linked diagrams. In addition, because of the computational efficiency of MBPT, calculations can be performed up to fourth order in the perturbation expansion and include single, double, triple, and quadruple excitations in the calculation of the correlation energy. Such calculations are often performed with a split valence plus polarization basis set. For the light element compounds which exhibit ionic bonding, the inclusion of diffuse basis functions and possibly higher polarization d or f-functions may be required for a quantitative treatment. Again, all of the necessary programs to handle expansions up to MP4 (SDTQ), with inclusion of up to f-functions are operational and in routine use at UTRC.

2.1.2 Density Functional Approach.

The X_α method (Reference 26) for the electronic structure of atoms, molecules, clusters and solids is a local potential model obtained by making a simple approximation to the exchange - correlation energy. Although this

14

method, as currently implemented, is less accurate than standard ab initio approaches, it is very useful for heavy-atom molecular systems. For such systems ($Z \gtrsim 30$), relativistic effects become increasingly important and their incorporation into density functional methods is much easier than into ab initio methods. If we assume a nonrelativistic Hamiltonian with only electrostatic interactions, it can be shown that the total energy E of a system can be written exactly (Reference 24) (in atomic units) as

$$
E = \sum_i n_i \left\langle u_i \left| -\frac{1}{2} \nabla_1^2 + \sum_\mu \frac{z_\mu}{r_{1\mu}} \right| u_i \right\rangle + \frac{1}{2} \sum_{\mu \neq \nu} \frac{z_\mu z_\nu}{r_{\mu\nu}}
$$

$$
+ \frac{1}{2} \sum_{ij} n_i n_j \left\langle u_i u_j \left| \frac{1}{r_{12}} \right| u_i u_j \right\rangle + E_{xc}
$$

(22)

This expression is exact provided the u_i are natural orbitals and n_i are their occupation numbers (i.e., eigenfunctions and eigenvalues of the first order density matrix). The first term in Equation (22) represents the kinetic and electron-nuclear energies. The second term is the nuclear repulsion energy. The sums (μ, ν) are over all the nuclear charges in the system. The third term is the electron-electron repulsion term, which represents the classical electrostatic energy of the charge density ρ interacting with itself, where

$$
\rho(1) = \sum_i n_i u_i^*(1) u_i(1)
$$

(23)

The last term E_{xc} represents the exchange correlation energy and can be expressed formally as

$$
E_{xc} = \frac{1}{2} \int \rho(1) \, d\vec{r}_1 \int \frac{\rho_{xc}(1,2)}{r_{12}} \, d\vec{r}_2 ,
$$

(24)

where $\rho_{xc}(1, 2)$ represents the exchange-correlation hole around an electron at position 1. In the exact expression, ρ_{xc} is dependent on the second-order density matrix. In the Hartree-Fock approximation E_{xc} is the exchange energy, ρ_{xc} represents the Fermi hole due to the exclusion principle and depends only

15

on the first-order density matrix. In the X_α method, we make a simpler assumption about ρ_{xc}. If we assume that the exchange-correlation hole is centered on the electron and is spherically symmetric, it can be shown that the exchange-correlation potential

$$U_{xc} = \int \frac{\rho_{xc}(1,2)}{r_{12}} \, d\vec{r}_2 \qquad (25)$$

is inversely proportional to the range of the hole, r_s, where r_s is defined by

$$\frac{4\pi}{3} \, r_s^3 \, \rho(1) = 1 \qquad (26)$$

Therefore, in the X_α model, the potential U_{xc} is proportional to $\rho^{1/3}(\vec{r})$. We define a scaling parameter α such that

$$U_{x_\alpha}(1) = -\frac{9\alpha}{2} \, (3\rho(1)/8\pi)^{1/3} \qquad (27)$$

The expression in Equation (27) is defined so that $\alpha = 2/3$ for the case of a free electron gas in the Hartree-Fock model (Reference 28) and $\alpha = 1$ for the potential originally suggested by Slater (Reference 29). A convenient way to choose this parameter for molecular and solid state applications is to optimize the solutions to the X_α equations in the atomic limit. Schwarz (Reference 30) has done this for atoms from $z = 1$ to $z = 41$ and found values between 2/3 and 1.

In the "spin polarized" version of the X_α theory, it is assumed (as in the spin-unrestricted Hartree-Fock model) that electrons interact only with a potential determined by the charge density of the same spin. In this case the contribution to the total energy is summed over the two spins, $s = ^+\!/- 1/2$.

$$E_{xc} = \frac{1}{2} \sum_s \int \rho_s(1) \, U_{x\alpha,s}(1) \, d\vec{r}_1 \qquad (28)$$

16

where the potential is spin-dependent

$$U_{x_{\alpha}, s}(1) = -\frac{9\alpha}{2} \left(3\rho_s(1)/4\pi\right)^{1/3} \tag{29}$$

and ρ_s is the charge density corresponding to electrons of spin s. The spin polarized X_α model is useful for describing atoms and molecules with open-shell configurations and crystals which are ferromagnetic or anti-ferromagnetic.

Once one has made the X_α approximation to the total energy functional E in Equation (22), then the rest of the theory follows from the application of the variational principle. The orbitals u_i are determined by demanding that E be stationary with respect to variations in u_i. This leads to the set of one-electron X_α equations

$$\left[-\frac{1}{2}\nabla_1^2 + \sum_{\mu} \frac{z_\mu}{r_{1\mu}} + \int \frac{\rho(2)}{r_{12}} d\vec{r}_2 + \frac{2}{3} U_{x\alpha}\right] u_i = \epsilon_i u_i \tag{30}$$

where ϵ_i is the one-electron eigenvalue associated with u_i. Since $\rho(\vec{r})$ is defined in terms of the orbitals u_i, Equation (30) must be solved iteratively, until self-consistency is achieved. Empirically, if one takes as an initial guess that ρ is approximately a sum of superimposed atomic charge densities, then the convergence of this procedure is fairly rapid. The factor of 2/3 multiplying the potential is a result of the linear dependence of E_{xc} on ρ. This also has a consequence that the X_α eigenvalues ϵ_i do not satisfy Koopman's theorem, i.e., they cannot be interpreted as ionization energies. However, it can be shown that the ϵ_i are partial derivatives of the total expression of Equation (22) with respect to the occupation number,

$$\epsilon_i = \frac{\partial E}{\partial n_i} \tag{31}$$

If E were a linear function of n_i, then Koopmans' theorem would hold. However, because of the dominant Coulomb term, E is better approximated by a quadratic function in n_i. This leads to the "transition state" approximation which allows one to equate the difference in total energy between the state (n_i, n_j) and $(n_i - 1, n_j + 1)$ to the difference in the one-electron

17

energies $\varepsilon_j - \varepsilon_i$ calculated in the state $(n_i - 1/2, n_j + 1/2)$. The error in this approximation is proportional to third-order derivatives of E with respect to n_i and n_j, which are usually small (Reference 31). The main advantage of using the transition state rather than directly comparing the total energy values is computational convenience, especially if the total energies are large numbers and the difference is small.

The relationship of Eq. (31) also implies the existence of a "Fermi level" for the ground state. This can be seen by varying E with respect to n_i under the condition that the sum $\sum_i n_i$ is a constant, i.e.,

$$\delta\left[E - \lambda \sum_i n_i\right] = 0 \qquad (32)$$

implies $\partial E/\partial n_i = \lambda$, where λ is a Lagrangian multiplier. This implies that the total energy is stationary when all the one-electron energies are equal. However, the occupation numbers are also subject to the restriction $0 \le n_i \le 1$. This leads to the following conditions on the ground state occupation numbers:

$$
\begin{aligned}
\varepsilon_i < \lambda \cdot) \cdot \ n_i &= 1 \\
\varepsilon_i > \lambda \cdot) \cdot \ n_i &= 0 \\
\varepsilon_i = \lambda \cdot) \cdot \ 0 &\le n_i \le 1
\end{aligned}
\qquad (33)
$$

In other words, the ground state eigenvalues obey Fermi statistics with λ representing the Fermi energy. It should be noted that, in contrast to the Hartree-Fock theory, where all the n_i are either 0 or 1, the X_α model predicts, in some cases, fractional occupation numbers at the Fermi level. In particular, this will occur in a system (such as transition metal or actinide atom) which has more than one open shell.

The X_α model differs in other significant ways from the Hartree-Fock method. In fact, the simplification introduced in approximating the total energy expression introduces several distinct advantages over Hartree-Fock:

1. The primary advantage is purely computational. The one-electron potential in Equation (30) is orbital-independent and local, i.e., it is the same for all electrons (except in the spin-polarized X_α theory) and is a multiplicative operator. On the other hand, the Hartree-Fock potential is

18

nonlocal, or equivalently, there is a different local potential for each orbital. This involves a great deal more computational effort, especially for systems described by a large number of orbitals. It has been shown (Reference 32) that the X_α orbitals for the first and second row atoms are at least as accurate as a double-zeta basis set, and are probably better for larger atoms which involve electrons with $\ell \geq 2$.

2. The orbital-independent X_α potential leads to a better one-electron description of electronic excitations of a system. Both the unoccupied $(n_i = 0)$ and occupied $(n_i = 1)$ eigenfunctions are under the influence of the same potential resulting from the other N-1 electrons. The Hartree-Fock virtual orbitals see a potential characteristic of the N occupied orbitals, and therefore are not as suitable for describing the excited states. Actually, although the ground state virtual eigenvalues are usually a good description of the one-electron excitations, the virtual spectrum of the transition state potential where one-half an electron has been removed from the system gives a much better first-order picture of these levels (Reference 33).

3. As has been shown by Slater (Reference 34), the X_α model rigorously satisfies both the virial and Hellman-Feynman theorems, independent of the value of the parameter α. This is convenient for calculating the force on a nucleus directly in terms of a three-dimensional integral, rather than the six-dimensional integrals in the expression for the total energy of Equation (22).

2.1.2.1 Computational Aspects of the X_α Method. In application of the X_α model to finite molecular systems, there are two practical aspects of the calculations which must be considered. The first concerns the choice of the integration framework for describing the molecular wavefunctions and the second deals with the choice of the exchange parameter, α, in different regions of space.

In computations with heteronuclear molecules, there are several free parameters that must be chosen: the ratio of sphere radii for the atomic spheres of integration at a given internuclear separation, the degree of sphere overlap, and the value of the exchange parameter in the atomic spheres and the intersphere region.

It has been found that changing the ratio of the sphere radii for the two atoms in a heteronuclear diatomic molecule introduces changes in the total energy that can be large on a chemical scale ($\sim$ 1 eV). A choice for sphere radii based on covalent bonding radii does not necessarily provide a good estimate for these calculations. The value of the exchange parameter, α, and the sphere radii and/or sphere overlap is normally fixed in X_α calculations for crystals where the geometry is fixed. However, to develop a potential curve, the molecule description needs to change substantially as the inter-nuclear separation varies and the changing sphere radii include varying frac-tions of the total molecular charge (Reference 35). Studies made at UTRC have shown that at any given separation the total energy calculated from the X_α model is a minimum at the radii ratio where the spherically averaged poten-tials from the two atomic centers is equal at the sphere radius.

$$V_1(r_{s_1}) = V_2(r_{s_2}) \tag{34}$$

This relationship between the potential match at the sphere boundary and the minimum in the total energy appears to hold exactly for "neutral" atoms and holds well for ionic molecular constituents. In the case of two ionic species, the long range tail of the potential must go like $+2/R$ for one ion and $-2/R$ (in Rydbergs) for the other ion and so at large internuclear separa-tions, the tails of the potential cannot match well. However, at reasonable separations, the $1/R$ character of the potential does not invalidate the poten-tial match criterion for radii selection. This match for the atomic poten-tials is applied to the self-consistent potentials.

In molecules with significant charge sharing in the bonds, the radii of the atomic spheres is frequently increased in X_α calculations so that an overlap region appears in the vicinity of the bond (Reference 36). Studies made at UTRC show that the contribution to the total molecular energy from the exchange integral shows a minimum at the optimum sphere radius or sphere over-lap. This provides a sensitive criterion for selecting these parameters.

The values of the exchange parameters in the spherical integration region around each atomic center are frequently set at the atomic values both for neutral and for ionic molecular constituents. However, for light atoms, the value of α which best reproduces Hartree-Fock results varies substantially with ionicity. In argon, the following table compares, for the neutral atom

20

and the positive ion, the HF energy and the X_α energy calculated for several values of α.

	α	$X\alpha$ Energy	HF Energy
Ar ^{0}	.72177	526.8176	526.8173
Ar$^{+1/2}$	.72177	526.5857	–
	.72213	526.6007	–
Ar^{+1}	.72177	526.2447	–
	.72213	526.2596	–
	.72249	526.2745	526.2743

The optimum value of α changes even more rapidly in the fluorine atom going from 0.73732 for F^0 to .72991 for F^{-1}. Since the total energy depends linearly on α, this parameter must be chosen carefully.

The intersphere exchange coefficient is chosen to be a weighted average of the atomic exchange parameters from the two constituents. At small internuclear separations, the optimum radius for an atomic sphere frequently places significant amounts of charge outside that atomic sphere – charge that is still strongly associated with its original center rather than being transferred to the other center or associated with the molecular binding region. To best account for these cases the weighting coefficients are chosen to reflect the origin of the charge in the intersphere (or outersphere region),

$$\alpha_{intersphere} = \frac{\alpha_{s_1}(Q_{s_1} - Q_1^{\,o}) + \alpha_{s_2}(Q_{s_2} - Q_2^{\,o})}{(Q_{s_1} - Q_1^{\,o}) + (Q_{s_2} - Q_2^{\,o})} \tag{35}$$

where $(Q_{s_i} - Q_i^{\,o})$ is the charge lost from sphere i relative to its atomic value (or ionic value) $Q_i^{\,o}$ and α_{s_i} is the atomic exchange parameter for sphere i. This value for $\alpha_{intersphere}$ is calculated dynamically – it is updated after each iteration in the self-consistent calculation.

While for heavy atoms, these changes in the exchange parameter would be small, the α's for small atoms vary rapidly with z (and with ionicity). The correct choice of the exchange parameters influences not only the total energy

calculated for the molecule but also in some cases affects the distribution of charge between the atomic spheres and the intersphere region.

2.1.3 Ab Initio Gaussian Wavefunctions.

Owing to the complexity of evaluating multicenter electron repulsion integrals over Slater-type (exponential) orbitals, various groups have adopted a computational approach to electronic structure calculations based on Gaussian orbitals. A highly developed program, named Gaussian 86, is available from Carnegie-Mellon University (Reference 21).

Gaussian 86 is a connected system of programs for performing ab initio molecular orbital (MO) calculations. It represents further development of the Gaussian 70, Gaussian 76, Gaussian 80 and Gaussian 82 systems already published. The contributors to the current version include: M. J. Frisch, J. S. Binkley, H. B. Schlegel, K. Raghavachari, C. F. Melius, R. L. Martin, J. J. P. Stewart, F. W. Bobrowicz, C. M. Rohlfing, L. R. Kahn, D. J. Defrees, R. Seeger, R. A. Whiteside, D. J. Fox, E. M. Fleuder, and J. A. Pople. Gaussian 86 was originally implemented on the chemistry department DEC VAX 11/780 computer at Carnegie-Mellon University. Since then this program has been installed on a number of different computers.

Gaussian 86 was designed with a transparent input data stream, making this program very user friendly. All of the standard input is free-format and mnemonic. Reasonable defaults for input data have been provided, and the output is intended to be self-explanatory. Mechanisms are available for the sophisticated user to override defaults or interface their own code to the Gaussian system. In this respect, we intend to utilize Gaussian 86 as a fundamental framework for several applications. Options are being incorporated into this code to provide capabilities beyond Hartree-Fock and various perturbation theory options.

The capabilities of the Gaussian 86 system include:

a) Calculation of one- and two-electron integrals over s, p, d, and f contracted gaussian functions. The basis functions can either be cartesian gaussians or pure angular momentum functions and a variety of basis sets are stored in the program and can be requested by name.

b) Self-consistent field calculations for restricted closed-shell (RHF), unrestricted open-shell (UHF), and open-shell restricted (ROHF)

Hartree-Fock wavefunctions as well as those types of multiconfigurational wavefunctions that fall within the Generalized Valence Bond-Perfect Pairing (GVB-PP) formalism.

c) Evaluation of various one-electron properties of the Hartree-Fock wavefunction, including Mulliken population analysis, multipole moments, and electrostatic fields.

d) Automated geometry optimization to either minima or saddle points, and numerical differentiation to produce force constants, polarizabilities, and dipole derivatives. This feature can be used to develop minimum energy reaction paths along a complicated many dimensional potential energy surface.

e) Correlation energy calculations using Møller-Plesset perturbation theory carried to second, third, or fourth order.

f) Correlation energy calculations using configuration interaction (CI) using either all double excitations (CID) or all single and double excitations (CISD).

g) Correlation energy calculations using coupled cluster theory with double substitutions (CCD).

h) Analytic computation of the nuclear coordinate gradient of the RHF, UHF, ROHF, GVB-PP, MP2, CID and RCISD energies.

i) Computation of force constants (nuclear coordinate second derivatives), polarizabilities, hyperpolarizabilities, dipole derivatives, and polarizability derivatives analytically for RHF and UHF enegies, and numerically for RHF, UHF, MP2, CID and UCISD energies.

j) Harmonic vibrational analysis.

k) Determination of intensities for vibrational transitions at the HF, MP2, and CI levels.

l) Testing the SCF wave functions for stability under release of constraints.

To widen the applicability of Gaussian 86 to open-shell molecular species, an option which incorporates a spin-projected variational CI expansion is currently under development. The programs for constructing the elements of the hamiltonian matrix can be taken from our standard DIATOM code.

Alternatively, CI wavefunctions can be constructed using the unitary group approach presently implemented in the GAMESS code.

2.2 TRANSITION PROBABILITIES.

The electronic and vibrational-rotational wavefunctions of a pair of states can be used to calculate transition probabilities. If two molecular states are separated in energy by an amount ΔE_{nm} = hcν (h = Planck's constant, c = velocity of light, ν = frequency in wave numbers), the semi-classical theory of radiation (References 37 and 38) yields for the probability of a spontaneous transition from an upper state n to a lower state m

$$A_{nm} = \frac{4}{3} \frac{\Delta E_{nm}^3}{\hbar^4 c^3} \frac{S_{nm}}{g_n} \tag{36}$$

Here A_{nm} is the Einstein coefficient for spontaneous transition from level n → m, g_n is the total degeneracy factor for the upper state

$$g_n = (2 - \delta_{\sigma, \Lambda'})(2S' + 1)(2J' + 1) \tag{37}$$

and S_{nm} is the total strength of a component line in a specific state of polarization and propagated in a fixed direction. A related quantity is the mean radiative lifetime of state n defined by

$$\frac{1}{\tau_n} = \sum_{m<n} A_{nm} \tag{38}$$

the summation being over all lower levels which offer allowed connections. The intensity of the emitted radiation is

$$I_{nm} = \Delta E_{nm} N_n A_{nm} \tag{39}$$

where N_n is the number density in the upper state n. This analysis assumes that all degenerate states at the same level n are equally populated, which will be true for isotropic excitation. The total line strength S_{nm} can be

24

written as the square of the transition moment summed over all degenerate components of the molecular states n and m:

$$S_{nm} = \sum_{i,j} \left| M_{ji} \right|^2 \tag{40}$$

where j and i refer to all quantum numbers associated collectively with upper and lower electronic states, respectively.

In the Born-Oppenheimer approximation, assuming the separability of electronic and nuclear motion, the wavefunction for a diatomic molecule can be written as

$$\psi'_{vJM\Lambda} = \psi'_{el}(\underset{\sim}{r}, R)\, \psi_v(R)\, \psi_{JM\Lambda}(\theta, \chi, \phi) \tag{41}$$

where $\psi^{i}_{el}(\underset{\sim}{r}, R)$ is an electronic wavefunction for state i at fixed inter-nuclear separation R, $\psi_v(R)$ is a vibrational wavefunction for level v and $\psi_{Jn\Lambda}(\theta, x, \phi)$ refers to the rotational state specified by electronic angular momentum Λ, total angular momentum J and magnetic quantum number M. The representation is in a coordinate system related to a space-fixed system by the Eulerian angles (θ, x, ϕ). The transition moment M_{ji} can be written, using the wavefunction given by Equation (41), as

$$M_{ji} = \int \psi^{j}_{v'J'\Lambda'M'} \left\{ \underset{\sim}{M}^e + \underset{\sim}{M}^n \right\} \psi^{j}_{v''J''\Lambda''M''}\, d\tau_e d\tau_v d\tau_r \tag{42}$$

The subscripts e, v and r refer to the electronic, vibrational and rotational wavefunctions, and $\underset{\sim}{M}^e$ and $\underset{\sim}{M}^n$ are the electronic and nuclear electric dipole moments, respectively. Integration over the electronic wavefunction, in the Born-Oppenheimer approximation, causes the contribution of the nuclear

moment M^n to vanish for $i \neq j$. The electronic dipole moment can be written (References 38 and 39) in the form

$$\underset{\sim}{M}^e = -\sum_k e \underset{\sim}{r}_k' = -\left\{ \sum_k e \underset{\sim}{r}_k \right\} \cdot \underset{\sim}{\mathfrak{D}}(\theta, \chi, \phi) \tag{43}$$

where the primed coordinates refer to the space fixed system, the coordinates r_k refer to a molecule-fixed system and $\underset{\sim}{}(\theta, \chi, \phi)$ is a group rotation tensor whose elements are the direction cosines related to the Eulerian rotation angles (θ, χ, ϕ). Using bracket notation, Equations (42) and (43) can be combined to yield for the transition moment

$$M_{ji} = M_{iv''J''\Lambda''M''}^{jv'J'\Lambda'M'} = \left\langle jv' \left| -\sum_k e \underset{\sim}{r}_k \right| iv'' \right\rangle \cdot \left\langle J'\Lambda'M' \left| \underset{\sim}{\mathfrak{D}}(\theta,\chi,\phi) \right| J''\Lambda''M'' \right\rangle \tag{44}$$

The matrix elements $\langle J' \Lambda' M' | (\theta,\chi,\phi) | J'' \Lambda'' M'' \rangle$ determine the group selection rules for an allowed transition and have been evaluated for many types of transitions (References 40-42). Summing Equation (44) over the degenerate magnetic quantum numbers M' and M'', we have from Equation (40)

$$S_{nm} = S_{mv''J''\Lambda''}^{nv'J'\Lambda'} = \mathcal{S}_{J''\Lambda''}^{J'\Lambda'} p_{mv''}^{nv'} \tag{45}$$

where $\mathcal{S}_{J''\Lambda''}^{J'\Lambda'}$ is the Hönl-London factor (References 43 and 44) and

$$p_{mv''}^{nv'} = \sum_{i,j} \left| \left\langle jv' \left| -\sum_k e \underset{\sim}{r}_k \right| iv'' \right\rangle \right|^2 \tag{46}$$

is the band strength for the transition. Combining Equations (37), (39) and (45), we have for the intensity of a single emitting line from upper level n:

$$I_{nm} = I_{mv''J''}^{nv'J'} = \frac{4}{3} N_{J'} \frac{\left[\Delta E_{mv''J''}^{nv'J'}\right]^4 S_{mv''J''\Lambda''}^{nv'J'\Lambda'}}{\hbar^4 c^3 \omega_n (2J'+1)} \qquad (47)$$

where $N_{J''}$ is the number density in the upper rotational state J' and $\omega_n = (2-\delta_{\sigma,\Lambda})(2S'+1)$ is the electronic degeneracy. Taking an average value of $E_{m\ v''J''}^{n\ v'J'}$ for the whole band, Equation (48) can be summed to yield the total intensity in the (v', v") band:

$$I_{mv''}^{nv'} = \sum_{J',J''} I_{mv''J''}^{nv'J'} = \frac{4}{3} N_{v'} \frac{\left[\overline{\Delta E}_{mv''}^{nv'}\right]^4 p_{mv''}^{nv'}}{\hbar^4 c^3 \omega_n} \qquad (48)$$

where $N_{v'} = \sum_{J'} N_{J'}$ is the total number density in the upper vibrational level v' and where we make use of the group summation property

$$\sum_{J''} S_{J''\Lambda''}^{J'\Lambda'} = (2J'+1) \qquad (49)$$

Comparing Equations (39) and (48), we have for the Einstein spontaneous transition coefficient of the band (v', v")

$$A_{mv''}^{nv'} = \frac{4}{3} \frac{\left[\Delta E_{mv''}^{nv'}\right]^3 p_{mv''}^{nv'}}{\hbar^4 c^3 \omega_n} \qquad (50)$$

Similarly, the lifetime of an upper vibrational level v' of state n can be written

$$\frac{1}{\tau_n} = \sum_{m<n} \sum_{v''} A_{mv''}^{nv'} \qquad (51)$$

27

where the summation runs over all v" for each lower state m. Equation (50) can be cast in the computational form

$$A_{mv''}^{nv'} (\sec^{-1}) = \frac{(21.41759 \times 10^9)}{\omega_n} \left[\Delta E_{mv''}^{nv'} (a.u.) \right]^3 p_{mv''}^{nv'} (a.u.) \tag{52}$$

where $\Delta E_{m\,v''}^{n\,v'}$ and $p_{m\,v''}^{n\,v'}$ are in atomic units. It is also often convenient to relate the transition probability to the number of dispersion electrons needed to explain the emission strength classically. This number, the f-number or oscillator strength for emission, is given by

$$f_{nm,v'v''} = \frac{mc^3 h^2}{2e^2 \left[\overline{\Delta E}_{mv''}^{nv'} \right]^2} A_{mv''}^{nv'} \tag{53}$$

The inverse process of absorption is related to the above development through the Einstein B coefficient. Corresponding to Equation (39), we have for a single line in absorption

$$\frac{I_{mn}}{I_{\nu}^0 \Delta x} = \int_{\text{line} (v''v'J''J')} K(\nu) d\nu = h\nu_{mn} N_m B_{mn} \tag{54}$$

where $K(\nu)$ is the absorption coefficient of a beam of photons of frequency ν and

$$B_{mn} = B_{mv''J''\Lambda''}^{nv'J'\Lambda'} = \frac{2\pi}{3\hbar^2 c} \frac{S_{mv''J''\Lambda''}^{nv'J'\Lambda'}}{\omega_m (2J''+1)} \tag{55}$$

is the Einstein absorption coefficient for a single line. Summing over all lines in the band (v", v'), assuming an average band frequency, we obtain

$$\frac{I_{mv''}^{nv'}}{I_{\nu}^0 \Delta x} = N_{v''} \frac{2\pi}{3\hbar^2 c \omega_m} p_{mv''}^{nv'} \overline{\Delta E}_{mv''}^{nv'} \tag{56}$$

where $N_{v''} = \sum_{J''} N_{J''}$ is the total number density in the lower vibrational state v''. Corresponding to Equations (52) and (53) we can define an f-number or oscillator strength for absorption as

$$f_{mn,v''v'} = \frac{2m \, \overline{\Delta E}_{mv''}^{nv'}}{3\hbar^2 e^2 \omega_m} \; p_{mv''}^{nv'} \tag{57}$$

In computational form, Equation (57) becomes

$$f_{mn,v''v'} = \frac{2}{3} \cdot \frac{\overline{\Delta E}_{mv''}^{nv'}(a.u.)}{\omega_m} \; p_{mv''}^{nv'}(a.u.) \tag{58}$$

where $\overline{\Delta E}_{m\,v''}^{n\,v'}$ and $p_{m\,v''}^{n\,v'}$ are in atomic units. Combining Equations (50) and (53) and comparing with Equation (58), we see that the absorption and emission f-numbers are related by

$$f_{mn,v''v'} = \left(\frac{\omega_n}{\omega_m}\right) f_{nm,v'v''} \tag{59}$$

Some caution must be observed in the use of f-numbers given either by Equation (53) or (57) since both band f-numbers and system f-numbers are defined in the literature. The confusion arises from the several possible band averaging schemes that can be identified.

An integrated absorption coefficient (density corrected) can be defined from Equation (56) as

$$S_{v''_,v'} = \frac{1}{P_c} \; I_{mv''}^{nv'} \epsilon \, N_{v''} \, B_{v''_,v'} \left(1 - \exp \frac{-hc\nu_{v''_,v'}}{kT}\right) \frac{h\nu_{v''_,v'}}{Pc^2} \tag{60}$$

where the exponential factor corrects for stimulated emission. Equation 60 can be written in terms of the absorption f-number as

$$S_{v'',v'} = \frac{\pi e^2}{mc^2} \frac{N_{v''}}{P} \left(1 - \exp \frac{-hc\nu_{v'',v'}}{kT} \right) f_{mn,v''v'} \tag{61}$$

Using $hc/k = 1.43880$ cm-K°, we obtain a computational formula for the integrated absorption coefficient as $S_{v'',v'}$ $(cm^{-2} atm^{-1})$ =

$$2.3795 \times 10^7 \left(\frac{273.16}{T(K°)} \right) \left(\frac{N_{v''}}{N_T} \right) \left(1 - \exp \frac{1.43880 \, \nu_{v''v'} (cm^{-1})}{T} \right) \cdot f_{mn,v''v'} \tag{62}$$

The total integrated absorption is found from

$$S_{TOTAL} = \sum_{v''} \sum_{v'} S_{v'',v'} \tag{63}$$

where, under normal temperature conditions, only the first few fundamentals and overtones contribute to the summations.

The developments given above are rigorous for band systems where an average band frequency can be meaningfully defined. Further approximations, however, are often made. For example, the electronic component of the dipole transition moment can be defined as

$$R_{ji}(R) = \left\langle j \left| -\sum_k e r_{\sim k} \right| i \right\rangle \tag{64}$$

30

This quantity is often a slowly varying function of R and an average value can sometimes be chosen. Equation (46) can then be written approximately in factored form as

$$p_{mv''}^{nv'} \simeq q_{v'v''} \sum_{i,j} \left| \bar{R}_{ji}(\bar{R}) \right|^2 \tag{65}$$

where $q_{v'v''}$, the square of the vibrational overlap integral, is called the Franck-Condon factor. R_{ji} is evaluated at some mean value of the internuclear separation R. In addition, it is sometimes possible to account for a weak R-dependence in $\underset{\sim}{M}^e$ by a Taylor series expansion of this quantity about some reference value, $R_{\alpha\beta}$, usually referred to the (0, 0) band. We have

$$R_{ji} \simeq R_{ji}^{\alpha\beta} \left[1 + a(R - R_{\alpha\beta}) + b(R - R_{\alpha\beta})^2 + \cdots \right] \tag{66}$$

Substituting into Equation (66) and integrating yields

$$p_{mv''}^{nv'} \simeq q_{v'v''} \sum_{i,j} \left| R_{ji}^{\alpha\beta} \left[1 + a(\overline{R_{v'v''} - R_{\alpha\beta}}) + b(\overline{R_{v'v''} - R_{\alpha\beta}})^2 + \cdots \right] \right|^2 \tag{67}$$

where

$$(\overline{R_{v'v''} - R_{\alpha\beta}}) = \frac{\left\langle v' \left| (R - R_{\alpha\beta}) \right| v'' \right\rangle}{\left\langle v' \mid v'' \right\rangle} \tag{68}$$

is the R-centroid for the transition and

$$(\overline{R_{v'v''} - R_{\alpha\beta}})^2 = \frac{\left\langle v' \left| (R - R_{\alpha\beta})^2 \right| v'' \right\rangle}{\left\langle v' \mid v'' \right\rangle} \tag{69}$$

is the R^2-centroid. Note that this last term differs (to second order) from the square of the R-centroid. An alternate procedure can be developed by evaluating Equation (64) at each R-centroid, $\overline{R}_{v'v''}$. Then

$$p_{mv''}^{nv'} \approx q_{v'v''}\sum_{i,j}\left|R_{ji}(R_{v'v''})\right|^2 \qquad (70)$$

Equation (70) assumes that the vibrational wavefunction product $\psi_{v'}\,\psi_{v''}$ behaves like a delta function upon integration,

$$\psi_{v'}\,\psi_{v''} = \delta(R-\overline{R}_{v'v''})\,\langle v'|v''\rangle \qquad (71)$$

The range of validity of Equation (70) is therefore questionable, particularly for band systems with bad overlap conditions such as oxygen Schumann-Runge. The range of validity of the R-centroid approximation has been examined by Fraser (Reference 45).

The final step in calculating transition probabilities is the determination of $R_{ji}(R)$, the electronic dipole transition moment, for the entire range of internuclear separations, R, reached in the vibrational levels to be considered. This can be expressed in terms of the expansion of Equation (14) as

$$R_{ji}(R) = \sum_{\mu\nu} c_\mu^{j*}\, c_\nu^i \,\left\langle \psi_\mu(R)\left|\underset{\sim}{M}^e\right|\psi_\nu(R)\right\rangle \qquad (72)$$

where $c_\mu^{\,j}$ and $c_\nu^{\,i}$ are coefficients for ψ_{el}^j and ψ_{el}^i, respectively.

An analysis similar to that yielding Equation (10) and (11) gives

$$\left\langle \psi_\mu(R)\left|\underset{\sim}{M}^e\right|\psi_\nu(R)\right\rangle =$$

$$\sum_p \epsilon_p \left\langle \theta_{M_S}\left|\mathcal{O}_S P\right|\theta_{M_S}\right\rangle\left\langle \prod_{k=1}^n \psi_{\mu k}(\underset{\sim}{r}_k,R)\left|\underset{\sim}{M}^e P\right|\prod_{k=1}^n \psi_{\nu k}(\underset{\sim}{r}_k,R)\right\rangle \qquad (73)$$

The spatial integral in Equation (73) reduces to one-electron integrals equivalent to overlap integrals, and the evaluation of Equation (73) can be carried out by the same computer programs used for Equation (11). Programs for evaluating $R_{ji}(R)$ in Equation (72) have been developed at UTRC and examples of their application have appeared in the literature (Reference 8).

For perturbed electronic systems, the transition dipole moment will have a strong R-dependence and R-centroid or other approximations will be invalid. A direct evaluation of Equation (46) would therefore be required using the fully-coupled system of electronic and vibrational wavefunctions to properly account for the source of the band perturbations.

SECTION 3

DISCUSSION OF RELATIVISTIC METHODS

For heavy atoms ($Z \gtrsim 30$), and molecular systems built from heavy atoms, relativistic effects become increasingly important and should be taken into account in the calculation of the radial wavefunctions. The implementation of relativistic effects into atomic and molecular computer codes is only fairly recent owing to the increased complexities introduced in the self-consistent field (SCF) procedure and the greatly increased computer time required for such calculations. Compared with the non-relativistic case, the Dirac-Hartree-Fock (DHF) method requires that two radial functions, G_{nlj}, corresponding to the large component and F_{nlj}, corresponding to the small component must be calculated for each of the two possible j values. Thus, the numerical work of a DHF relativistic treatment is increased by nearly a factor of four over the nonrelativistic case, exclusive of increased complexities in evaluation of the terms of the Hamiltonian. In view of this, methods that have been developed to date for molecular systems have involved the use of model potentials to represent relativistic effects.

In the calculation of the internal energy of a molecular system comprised of n electrons and N nuclei, and considering only electrostatic interactions between the particles, we have for the total Hamiltonian

$$\mathcal{H} = \mathcal{H}_{el} - \sum \frac{\hbar^2}{2m_\alpha} \nabla_\alpha^2 + \frac{\hbar^2}{2 M_T} \left[\sum_{\substack{\beta=1 \\ \alpha \neq \beta}}^{N} \sum_{\alpha=1}^{N} \nabla_\alpha \cdot \nabla_\beta \right.$$
$$\left. + 2 \sum_{\alpha=1}^{N} \sum_{i=1}^{n} \nabla_\alpha \cdot \nabla_i + \sum_{i=1}^{n} \sum_{\substack{j=1 \\ i \neq j}}^{n} \nabla_i \cdot \nabla_j \right] \tag{74}$$

where

$$\mathcal{H}_{el} = - \frac{\hbar^2}{2 m_e} \sum_{i=1}^{n} \nabla_i^2 + V^{el}(\underline{r}_n, \underline{R}_N) \tag{75}$$

34

where m_e, m_α, M_T, are the masses of the electron, atom α and combined system mass, respectively. Now since the ratios m_e/m_α and m_e/M_T are both small, $(2 \times 10^{-6} - 5 \times 10^{-4})$ we can effect a separation of the electronic and nuclear coordinates treating the total wavefunction as a product of a nuclear and an electronic part. We have

$$\psi(\underset{\sim}{r}_n, \underset{\sim}{R}_N) = \sum_k \chi_k(\underset{\sim}{R}_N) \psi_k(\underset{\sim}{r}_n, \underset{\sim}{R}_N) \tag{76}$$

where $\psi_k(\underset{\sim}{r}_n, R_N)$ is an electronic wavefunction parametric in the nuclear coordinates as given in Equation (76) and $\chi_k(\underset{\sim}{R}_N)$ are nuclear motion wavefunctions which satisfy (neglecting terms of the order of m_e/m_α)

$$\left[-\sum_{\alpha=1}^{N} \frac{\hbar^2}{2m_\alpha} \nabla_\alpha^2 + \frac{\hbar^2}{2M_T} \sum_{\substack{\alpha=1 \\ \alpha \neq \beta}}^{N} \sum_{\beta=1}^{N} \nabla_\alpha \cdot \nabla_\beta + V^{el}(\underset{\sim}{r}_n, \underset{\sim}{R}_N) \right] \chi_k = i\hbar \frac{\partial \chi_k}{\partial t} \tag{77}$$

The cross term in $\nabla_\alpha \cdot \nabla_\beta$ can be eliminated by a proper change of variables and Equation (77) then reduces to a 3N-3 dimensional Schrödinger equation.

For most systems, where the velocity of motion of the nuclei is slow relative to the electron velocity, this decoupling of electronic and nuclear motion is valid and is referred to as the adiabatic approximation. Equation (76) thus defines an electronic eigenstate $\psi_k(\underset{\sim}{r}_n, \underset{\sim}{R}_N)$, parametric in the nuclear coordinates, and a corresponding eigenvalue $E_k(\underset{\sim}{R}_N)$ which is taken to represent the potential energy curve or surface corresponding to state k.

In the usual ab initio method for calculating the electronic properties of a molecular system, one starts from a zero-order Hamiltonian that is exact except for relativistic and magnetic effects, and which involves the evaluation of electronic energies and other relevant quantities for wavefunctions that are properly antisymmetrized in the coordinates of all the electrons.

For a system containing n electrons and M nuclei, the zero-order Hamiltonian depends parametrically on the nuclear positions and is of the form

$$\mathcal{H}_e = -\frac{1}{2}\sum_{i=1}^{n}\nabla_i^2 - \sum_{i=1}^{n}\sum_{j=1}^{M}\frac{z_j}{|\vec{r}_i - \vec{R}_j|} + \sum_{1 \leq i < j}^{M}\frac{z_i z_j}{|\vec{R}_i - \vec{R}_j|} + \sum_{1 \leq i < j}\frac{1}{|\vec{r}_i - \vec{r}_j|} \tag{78}$$

where z_i and $\vec{R}_i$ are the charge and position of nucleus i, $\vec{r}_j$ is the position of electron j, and ∇_j^2 is the Laplacian operator for electron j. All quantities are in atomic units, i.e. lengths in bohrs, energies in hartrees (1 hartree = 2 Rydbergs).

In addition to the electrostatic contribution, $\mathcal{H}_e$, the complete Hamiltonian should contain additional terms which correct for magnetic interactions and relativisitic effects. These correction terms may be of importance in several applications. These include:

(1) calculation of the probability of making a transition from one quantum state to another in high-momentum collisions such as those that can occur in hot atom or heavy atom chemical dynamics experiments;

(2) determination of the interaction energy in heavy nuclei systems such as Cs_2 and UO^+, which exhibit open-shell structure on both nuclei at infinite internuclear separations;

(3) calculation of the intermolecular forces between free radicals, electronically excited states of molecules with open-shell structure, and long molecular conformations of possible biological interest.

3.1 BREIT-PAULI HAMILTONIAN.

The relativistic correction terms to the usual electrostatic Hamiltonian have been derived through order α^2, where α is the fine structure constant, and are often referred to as the Breit-Pauli (Reference 46) Hamiltonian terms. This Hamiltonian has been derived by Bethe and Salpeter (Reference 47) for a two-electron system and has been generalized to the many-electron system by Hirschfelder, et al (Reference 48) and Itoh (Reference 49). In the absence of external electric or magnetic fields we can represent these correction terms

as follows. Let $\vec{s}_j$ and $\vec{p}_j = \frac{1}{i}\Delta_j$ denote the operators for the spin and linear moment of electron j, respectively. Then the generalized Breit-Pauli Hamiltonian, correct to terms of $\mathcal{O}(\alpha^2/M)$, can be written as:

$$\mathcal{H}_{BP} = \mathcal{H}_e + \mathcal{H}_{LL} + \mathcal{H}_{SS} + \mathcal{H}_{LS} + \mathcal{H}_p + \mathcal{H}_D \tag{79}$$

where $\mathcal{H}_e$ is given by Equation (78) and the correction terms can be expressed as follows:

$$\mathcal{H}_{LL} = -\frac{1}{2} \sum_{1 \le k \le j} \frac{1}{r_{jk}^3} \left[r_{jk}^2 \ \vec{p}_j \cdot \vec{p}_k + \vec{r}_{jk} \cdot (\vec{r}_{jk} \cdot \vec{p}_j) \, p_k \right] \tag{80}$$

$$\mathcal{H}_{SS} = \sum_{1 \le k < j} \left\{ -\left(\frac{8\pi}{3}\right) \vec{s}_j \cdot \vec{s}_k \ \delta(\vec{r}_{jk}) \right.$$
$$\left. + \frac{1}{r_{jk}^5} \left[r_{jk}^2 \ (\vec{s}_j \cdot \vec{s}_k) - 3 (\vec{s}_j \cdot \vec{r}_{jk})(\vec{s}_k \cdot \vec{r}_{jk}) \right] \right\} \tag{81}$$

$$\mathcal{H}_{LS} = \frac{1}{2} \sum_{\alpha} \sum_{j} \left(\frac{z_\alpha}{r_{j\alpha}^3}\right) (\vec{r}_{j\alpha} \cdot \vec{p}_j) \cdot \vec{s}_j$$
$$-\frac{1}{2} \sum_{1 \le k \le j} \frac{1}{r_{jk}^3} \left[(\vec{r}_{jk} \times \vec{p}_j) \cdot \vec{s}_j - 2 (\vec{r}_{jk} \times \vec{p}_k) \cdot \vec{s}_j \right] \tag{82}$$

$$\mathcal{H}_p = -\frac{1}{8} \sum_{j} p_j^4 \tag{83}$$

$$\mathcal{H}_D = \frac{\pi}{2} \left[\sum_{\alpha} \sum_{j} z_\alpha \ \delta(\vec{r}_{j\alpha}) - 2 \sum_{1 \le k < j} \delta(\vec{r}_{jk}) \right] \tag{84}$$

The first correction term, $\mathscr{H}_{LL}$, represents the magnetic orbit-orbit coupling terms of the electrons arising from the interaction of the magnetic fields created by their motion. The second term, $\mathscr{H}_{SS}$, gives the spin-spin magnetic coupling terms which are often quite appreciable. For $r_{jk} = 0$, only the delta-function contribution survives which represents the Fermi-contact spin interaction. The third term, $\mathscr{H}_{LS}$, is usually the largest in magnitude and represents the spin-orbit interaction between the spin and magnetic moment of each electron and the spin-other orbit interaction, which represents the coupling of the spin of one electron with the magnetic moment of a different electron. The term, $\mathscr{H}_p$, corrects for variation of the electron mass with velocity and the term, $\mathscr{H}_D$, represents electron spin terms identified by Dirac which appear to have no classical analogue.

Aside from the spin-orbit term, $\mathscr{H}_{LS}$, usually only the last term, $_D$, (often called the Darwin correction term) and $\mathscr{H}_p$, the mass-velocity term, are retained in the Hamiltonian, yielding the so-called Pauli approximation (Reference 47).

The eigenfunctions of the Hamiltonian represented by Equation (79) are four-component Dirac spinors which may be expressed as:

$$r \psi_{nkm} = \begin{pmatrix} P_{nk}(r) \; \chi_{km}(\theta,\phi) \\ iQ_{nk}(r) \; \chi_{-km}(\theta,\phi) \end{pmatrix} \tag{85}$$

where $\chi_{km}(\theta, \phi)$ are products of spherical harmonics and Pauli spinors and $P_{nk}(r)$, $Q_{nk}(r)$ represent, respectively, the large and small components of the radial wave equation. The exact solution of the Breit-Pauli Hamiltonian has only been given for one- and two-electron atomic systems (Reference 47) owing to the complexity of the operators for the general n-electron case. For a molecular system, Kolos and Wolniewicz (Reference 50) have calculated the relativistic corrections to H_2 using Equation (79) to $\mathcal{O}(\alpha^2)$. No heavier molecular systems have been treated using the full Breit-Pauli Hamiltonian.

3.2 APPROXIMATE TREATMENTS.

Although the Breit-Pauli Hamiltonian given in Equation (79) can formally be employed in a molecular system, both the multiplicity of terms and the

difficulty of evaluation of the resultant molecular integrals has precluded its general use to date. For atomic systems, various approximate methods of solution, within a Hartree-Fock or multiconfiguration Hartree-Fock framework, have been proposed for atoms (References 51-55). In most of these methods, a restricted Hamiltonian which includes only the one-electron Dirac terms is usually employed. The contributions of the Breit operators for spin-magnetic interactions and velocity retardation are then calculated as first-order perturbations using the zeroth-order Dirac relativistic wavefunctions.

An even more approximate method for incorporating the major relativistic effects has been proposed by Cowan and Griffin (Reference 56). In this method, the mass-velocity($\mathcal{H}_p$) and Darwin($\mathcal{H}_D$) terms, written in terms of the Pauli equation for one-electron atoms, are simply added to the usual non-relativistic Hamiltonian operator. In addition, the spin-orbit terms, , , are omitted, thereby reducing the system of equations to a single form representing the description of the major component wavefunction, $P_{nk}(r)$, evaluated at the center-of-gravity of the spin-orbit states. The rationale for this approximation lies in the observation that detailed atomic calculations using the complete DHF method have indicated that, even for an atom as heavy as uranium, less than 1 percent of the total charge is described by the small component radial wavefunctions.

The resulting equations have the form:

$$\left[-\frac{d^2}{dr^2} + \frac{\ell_i(\ell_i+1)}{r^2} + v^i(r) + H_m^i(r) + H_D^i(r) \right] G_{n\ell}^i(r) = \epsilon_{n\ell}^i G_{n\ell}^i(r) \tag{86}$$

where the mass-velocity and Darwin terms take the form

$$H_m^i(r) = -\frac{\alpha^2}{4} \left[\epsilon^i - v^i(r) \right]^2 \tag{87}$$

$$H_D^i(r) = -\delta_{\ell_i,0} \frac{\alpha^2}{4} \left[1 + \frac{\alpha^2}{4} (\epsilon^i - v^i(r)) \right]^{-1} \left[\frac{dv^i(r)}{dr} \left(\frac{d}{dr} - \frac{1}{r} \right) \right] \tag{88}$$

and $\alpha \simeq 1/137.036$ is the fine structure constant. The spin-orbit term is omitted in Equation (86) and thus these equations represent center of gravity radial functions averaged over the two possible total angular momentum quantum numbers. Equation (86) represents (apart from the neglect of spin-orbit effects) the relativistic corrections to first order in α^2. A more accurate analysis of heavy atom energy levels and spectra is available through the use of the radial functions, $G^i_{nl}(r)$, found from Equation (86), and a first-order perturbation calculation. Cowan and Griffin (Reference 56) have illustrated the utility and accuracy of such an approach.

Recently, Wood and Boring (Reference 57) have adapted this approximate relativistic method to the local exchange problem and have implemented the solution of Equation (86) within the context of the multiple scattering $X\alpha$ method (Reference 26). The central field Hamiltonian is modified to include mass-velocity and Darwin terms, given by Equations (87) and (88), in the sphere surrounding each atomic center. The intersphere region in the multiple scattering approach (constant potential region) is treated nonrelativistically since charge in this region is far from a nucleus and is screened by the charge concentrated around the atomic centers. The matching conditions for continuity of the wavefunction at the sphere boundaries permits any necessary charge transfer between the relativistic intra-atomic regions and the nonrelativistic interatomic constant potential regions. For an atom, the Wood-Boring treatment reduces to the Dirac-Slater local exchange method, but with the neglect of spin-orbit terms.

The implementation of Equation (86) into existing nonrelativistic multiple scattering molecular codes is facilitated by a change in the dependent variable, $G^i_{nl}(r)$, to eliminate the first derivative of the wavefunction, illustrated in Equation (88). The usual Numerov method of solution can then be applied to the central field problem; the only new requirement being the numerical tabulation of the first and second derivatives of the potential at each grid point in the integrations. These derivatives are computed only once for each complete SCF cycle and thus the total required computer time for a typical problem is not significantly increased as compared with a nonrelativistic calculation. A complete self-consistent program incorporating this method has been developed at UTRC. Our code has been tested by repeating calculations for the U and Pu atoms (Reference 56), where we find excellent agreement with the more exact, but cumbersome, Dirac-Slater calculations.

Results for molecular calculations have recently been reported by Boring and Wood for UF_6 and UO_2^{++} (References 58 and 59). These calculations were carried out to illustrate the shifts in the valence levels for such systems resulting from relativistic effects. The total energy was not of principal concern.

We have recently reported (Reference 60) the first all-electron calculation of the potential energy curves for a molecule (Hg_2^+) built from atoms which exhibit significant relativistic effects. This study illustrated that reliable total energies are obtainable through a relativistic multiple scattering density functional treatment, provided care is taken to optimize potential match and overlap criteria for such systems. This study formed the basis of the computational scheme that we have employed here for the uranium/oxygen system.

3.3 EFFECTIVE CORE MODELS.

It is well known from chemical experience that the outermost valence electrons contribute most to determining the chemical properties, especially spectroscopic properties, of molecules. The core electrons remain essentially unchanged from their atomic form except for internuclear separations of the order of the charge radii of the outer core region or less, wherein core polarization effects may become important. Since the computational time required for ab initio calculations of electronic structure goes up at least quadratically with the number of electrons in the system, there have been many attempts to replace the more tightly bound core electrons with simple one-electron effective potentials (References 61-69). Concurrent with elimination of an explicit treatment of the core electrons, a transformation of the valence orbital basis is required to insure that the lowest valence orbital of each symmetry has a nodeless radial form, since it is well known that the lowest energy eigenfunction for a local potential must be nodeless (Reference 70).

Typical of the several effective core models that have been reported is that due to Kahn, et al (Reference 68) whereby an effective core potential is described in terms of angularly dependent projection operators as

$$U^{core} = U_L^{core}(r) + \sum_l \sum_m |lm> \left[U_l^{core}(r) - U_L^{core}(r) \right] <lm| \qquad (89)$$

where L is taken at least as large as the highest angular momentum orbital occupied in the core. The term $U_L^{core}(r)$ represents the effective Coulomb and exchange potential felt by the valence electrons. The second term essentially accounts for the repulsive potential between valence and core electrons for each symmetry ℓ. The only non-local character exhibited by a potential of the form of Equation (89) arises from the ℓ-dependence which can be cast in terms of one-electron integrals between the core and valence orbitals. Explicit two-electron terms connecting core and valence orbitals are thus avoided which greatly simplifies the calculation of matrix elements of the effective Hamiltonian. The potential given by Equation (89) can be compared with the generalized Phillips-Kleinman pseudo-potential (Reference 63).

$$U^{core} = \sum_{c} (2 J_c - K_c) + V^{CO} \tag{90}$$

where J_c and K_c represent the core orbital Coulomb and exchange operators and V^{CO} is a complicated non-local operator which guarantees core-valence orthogonality. Since the P-K core orbitals must simultaneously be eigenfunctions of both the core and valence Hartree-Fock Hamiltonians, V^{CO}, in general, contains complicated two-electron terms and limits the usefulness of Equation (90) over a full ab initio treatment.

The prescription of Kahn can be implemented by analytically fitting a nodeless pseudo-orbital, $\chi_{n\ell}$, to a linear combination of numerical or analytic Hartree-Fock orbitals determined from a full self-consistent treatment of the core electrons, using, for example, the multiconfiguration Hartree-Fock code of Froese-Fischer (Reference 71). The components, $U_\ell^{core}(r)$, of Equation (89) are then defined implicitly from the Schrödinger equation

$$\left[-\frac{\nabla^2}{2} - \frac{z}{r} + U_\ell^{core}(r) + 2 J_{val} - K_{val} \right] \chi_{n\ell} = \epsilon_{nl} \chi_{n\ell} \tag{91}$$

whereby

$$U_l{}^{core}(r) = \epsilon_{nl} + \frac{z}{r} + \frac{1}{X_{nl}} \left[\frac{\nabla^2}{2} - 2 J_{val} + K_{val} \right] X_{nl} \qquad (92)$$

Equation (91) can be extended to relativistic systems in several ways. Kahn, et al (Reference 72) suggest an approximate treatment of adding only the mass-velocity and Darwin terms to the usual electrostatic Hamiltonian and to determine approximate HF orbitals in the manner prescribed by Cowan and Griffin (Reference 56). Equation (91) is then used to determine an effective $U_l{}^{core}$ (r) such that ϵ_{nl} are the eigenvalues of the CG approximate relativistic solution and X_{nl} are curve-fitted to the CG-HF orbitals. In this treatment, the X_{nl} represent approximate solutions to the major component wavefunction, P_{nl}, determined at the center-of-gravity of the spin-orbit states.

Lee, et al (Reference 69) adopt a somewhat more complicated treatment in which the spin-orbit operator is added to the usual electrostatic Hamiltonian, in addition to the mass-velocity and Darwin terms retained in the Cowan-Griffin treatment. The large component eigenfunctions of a full Dirac-Hartree-Fock treatment of the atom, as given, for example, by Desclaux (Reference 73) are then curve-fitted in a manner similar to the Kahn treatment but include the additional index for the particular spin-orbit state, X_{nlj}. Use of these eigenfunctions in a molecular system fits more naturally into a (J-J) coupling scheme whereas the X_{nl} determined using the Kahn method are more easily represented using Λ-s coupling.

Although these effective core models can often accurately describe an atomic eigenvalue sequence, including even high-lying electronically excited states (Reference 74), there are inherent difficulties in their application to molecular environments, where the maximum angular momentum component of the valence shell orbitals may often exceed the highest l-value component retained in Equation (92). This is particularly true for valence orbitals which exhibit strong changes from atomic form through hybridization with higher angular momentum orbitals or through the addition of more compact polarization terms. In either case, since the relativistic terms are now all buried in a fixed rather than a dynamic relativistic operator, only static core effects are

43

imposed in determining the shape of the valence molecular orbitals. Relativistic effects between valence electrons and shielding effects of the core by the valence electrons are therefore neglected in these effective core treatments. In addition, the models obviously break down completely when the nuclei are brought together to dimensions such that core overlap and polarization effects become significant. Unfortunately, calculations to date seem to indicate that such effects begin to set in for internuclear separations of the order of equilibrium bond lengths.

SECTION 4

DISCUSSION OF RESULTS

An analysis of the electronic structure of UO and UO$^+$ using a relativistic formulation has previously been undertaken by UTRC (References 75 and 76). Preliminary calculations were performed for several states of UO and UO$^+$ and for the ground state of UO_2, UO_2^+ and UO_2^{++}. In addition, an analysis of the electronic structure of the ground state of TiO$^+$ indicated the unexpected result that this system is a weak LWIR radiator. A data base for U$^\circ$, U^{+1} and U^{+2} has been collected for examining the role of dielectronic recombination as a charge neutralization mechanism in the uranium/oxygen system. A preliminary analysis of dielectronic recombination of e + U$^+$ and e + U^{++} has been carried out. Finally, a study of the N + O_2 reaction to form vibrationally excited NO has been undertaken. A brief summary of the results of these calculations follows.

4.1 UO.

Electronic structure calculations were carried out for this system using a relativistic density functional formalism. Only a selected group of symmetries was studied. Our calculations indicate that the lowest symmetry of UO is derived from the (Λ,S) coupled ^{5}I state and has the following principal molecular orbital occupancy:

$$^5I \left[1\sigma^2\ 2\sigma^2\ 3\sigma^2\ 4\sigma^2\ 1\pi^4\ 2\pi^4\ \vdots\ 3\pi\ 1\delta\ 1\phi\ \vdots\ 5\sigma \right] \qquad (93)$$
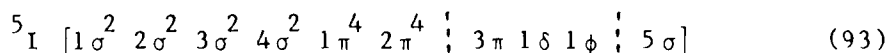
The $\vdots\ 3\pi\ 1\delta\ 1\phi\ \vdots$ group derives from the $5f^3$ atomic configuration in the U atom and is quartet coupled. We have found that the ^{5}I state of UO is the ground state but that several other symmetries, including ^{5}K and ^{3}I, are low-lying. Our results indicate that only states of triplet or quintet multiplicity are bound for this system. An examination of the structure of these low-lying states of UO indicates a near total charge transfer to U^{+2}O^{-2} for short (equilibrium) internuclear separations. This would yield 42 bound molecular states arising from U$\left[^5L \right]$ + O$\left[^3P \right]$ and 39 repulsive states. Since (J-J) coupling is surely a better approximation for UO, these two manifolds of

states will be optically connected and many pre-dissociation paths of the type:

$$UO^{*\ddagger} + h\nu \rightarrow UO^{**} \rightarrow U + O \qquad (94)$$
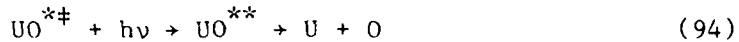
are possible. Here $UO^{*\ddagger}$ is a vibrationally excited low-multiplet state of UO and UO^{**} is a dissociating state. The predicted optical absorption should be strong since the transfer is from highly ionic states to neutral valence states of UO. Since UO has a large dissociation energy (7.87 eV), both one photon and two photon solar excitation processes are possible.

A vibrational analysis of the $\Omega = 5$ ground state of UO was carried out using a Hulbert-Hirshfelder (Reference 77) fit to our calculated potential curves. This fit yields an equilibrium internuclear distance of 1.89 Å and a fundamental vibrational constant (ω_e) of 859 cm^{-1}. The spin-orbit interaction was calculated using U^{+2} atomic splitting parameters. No explicit two-center effects are included. Our calculated spectroscopic data are compared in Table 1 with the theoretical work of Krauss and Stevens (Reference 78), the recent rotationally resolved experimental studies of Heaven and Nicolai (Reference 79), the recent rotational analysis reported by Kaledin, et al (Reference 80), and estimates based on experimental data for similar systems. The agreement is well within the uncertainty of the calculations or experimental estimates. The theoretical studies predict a $^5I_5$ or $^5I_4$ ground state for UO whereas the experimental data of both Heaven and Nicolai and Kaledin, et al suggest a $^5I_4$ ground state. Recent ligand field model calculations by Dulick (Reference 81) predict a $^5I_1$ ground state for UO, in substantial disagreement with previous theory and experiments. The crystal field model totally neglects overlap and back charge transfer effects in the $U^{+2}O^{-2}$ model, both of which have been found to be of importance in more exact studies carried out within a full molecular framework. The character of all of the low-lying multiplets of UO is similar however, and this apparent discrepency should not affect our conclusions about optical or LWIR absorptions.

An analysis of the LWIR emission from UO was carried out based on a ground ^5I electronic state. These calculations should also be representative of the LWIR emission from other low-lying electronic states since they exhibit similar ionicities. Our calculated f-numbers, including fundamentals and overtones, were reported in DNA-TR-82-159 (Reference 75). These data

46

$(v' > v'')$ were given for the lowest 30 vibrational levels. For UO, our calculated f-number for the 1-0 transition is 4.86×10^{-5} at $\lambda = 12.04$ μ.

4.2 UO$^+$.

Detailed searches of several symmetries of UO$^+$ were carried out to determine the ground molecular state of this system. Our calculations indicate that the lowest symmetry of UO$^+$ is derived from the (Λ, S) coupled ^{4}I state and has the following principal molecular orbital occupancy:

$$^4\text{I} \left[1\sigma^2\ 2\sigma^2\ 3\sigma^2\ 4\sigma^2\ 1\pi^4\ 2\pi^4\ \vdots\ 3\pi\ 1\phi\ 1\delta\ \vdots \right] \tag{95}$$
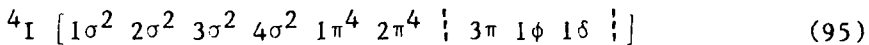
Again we found that the $\vdots\ 3\pi\ 1\phi\ 1\delta\ \vdots$ group is quartet coupled in the ground state but a second manifold of states for the UO$^+$ system, which exhibit doublet coupling of these electrons, lies about 2 eV above the ground state. An apparent gap in the density of states for UO$^+$ is found between these two groups. Calculations for UO$^+$ proved to be much more complex than UO owing to the presence of at least two low-lying dissociation limits of U$^+$ + O. In a molecular framework, the ionic U^{++}O$^-$ and U^{+3}O^{-2} structures will mix in all multiplicities with molecular ion states arising from U$^+[^4\text{I}]$ + O$[^3\text{P}]$, U$^+[^6\text{L}]$ + O$[^3\text{P}]$, and U$^+[^6\text{K}]$ + O$[^3\text{P}]$.

A vibrational analysis of the $\Omega = 9/2$ ground state of UO$^+$ was carried out using a Hulbert-Hirschfelder (Reference 77) fit to our calculated potential curves. The spin-orbit splittings were derived from atomic parameters for the U^{+3} ion. This fit yields an equilibrium internuclear distance of 1.84 Å and a fundamental vibrational constant of 890 cm^{-1}. These data are compared in Table 1 with other calculated estimates, since there are no experimental data available. The agreement between our work and that of Krauss and Stevens (Reference 78) is less satisfactory than in the case of UO but still well within the uncertainty of the several calculations.

A perturbative treatment for calculating the density of states in uranium molecules is available through the use of ligand field theory. Recent studies by Dulick predict that the ground state of UO$^+$ has $\Omega = 3/2$, in contrast to the effective core hamiltonian calculations of Krauss and Stevens (Reference 78) and our relativistic density functional calculations, both of which predict that the ground state has $\Omega = 9/2$. Again, the neglect of important molecular

effects in the ligand field model apparently results in a bias toward lower Ω values. Our calculated spin-orbit splitting for the 5f electrons in $U^{+3} \rightarrow U^{+5}$ is given in Table 2 where a comparison with earlier studies by Wood and Boring (Reference 57) is given. The overall agreement for these atomic ions is excellent. We have carried out calculations of the excitation energies of several configurations of U^{+3}. These data clearly indicate that the ^4I component of $5f^3$ is low-lying and that the lowest doublet manifold lies ~ 2.2 eV above the ground state. If this splitting carries over to the UO^+ ion without much change, the following solar pumped process is possible:

$$UO^+ \left[{}^4I \right] + h\nu \rightarrow UO^{+*} \left[{}^2H \right] \qquad (96)$$

$$e + UO^{+*} \left[{}^2H \right] \rightarrow U \left[{}^5L \right] + O \left[{}^3P \right] \qquad (97)$$
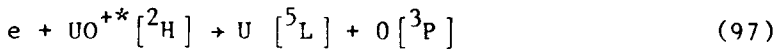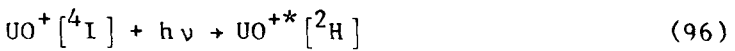
Dissociative-recombination is not energetically possible from the ground ^4I state of UO^+ but it is possible from the excited ^2H and higher states. The optical connections between the manifolds of UO^+ states will be studied in future work.

An analysis of the emission characteristics for the ground state of UO^+ indicates an oscillator strength for emission (f_{10}) of 5.17×10^{-5} at $\lambda = 11.3$ μ. A complete analysis of our calculated LWIR emission for UO^+ was given in DNA TR-82-159 (Reference 75). Our calculated LWIR emission for UO^+ is typical of that for a highly ionic metal oxide. We predict strong emission from the fundamentals of UO^+ in the wavelength region $11 \sim 14$ μ. Since this system exhibits weak anharmonicity, we find the overtones down in intensity by several orders of magnitude. However, the first excited state of UO^+ (^4H) lies at ~ 2800 cm^{-1} in our calculations with a predicted electronic oscillator strength of $\sim 1 \times 10^{-5}$ for the $^4I - {}^4H$ transition. The electronic and vibrational manifolds for UO^+ are highly overlapped above the second vibrational level of the ground $^5I_{9/2}$ state. Since the density of electronic states of UO^+ is very large above ~ 2.2 eV, we predict that strong solar pumping, followed by intense radiation in the region $0.6 \stackrel{\sim}{<} \lambda \stackrel{\sim}{<} 11.3$ μ should occur for this system. This conclusion is similar to that reached by Krauss and Stevens (Reference 78) based on their MCSCF analysis of the UO^+ system. Since the excited electronic states of UO^+ lying in the region of strong solar flux (.4 − .7 μ) exhibit shifted equilibrium internuclear separation from that of the ground ^4I state, we predict efficient conversion of solar photons to IR photons for this system.

48

4.3 UO_2^+.

An analysis of UO_2^+ has been carried out in $D_{\infty h}$ symmetry. McGlynn and Smith (Reference 82) have proposed a $^2\phi_u$ ground state for this ion based on simple molecular orbital arguments. Their set of one-electron orbital energies is based on a maximum overlap criterion that is empirical in character. More modern calculations of the actinide series atoms suggest that a $U^{+5}[0^{-2}]_2$ or $U^{+3}[0^{-1}]_2$ structure should be the most stable configuration. In terms of MO's, the lowest predicted electronic state ($D_{\infty h}$) would be:

$$1\sigma g^2 \ 1\sigma u^2 \ 2\sigma g^2 \ 1\pi u^4 \ 2\sigma u^2 \ 3\sigma g^2 \ 2\pi u^4 \ 1\pi g^4 \ 3\sigma u^2 \ \big| \ 1\phi u : {}^2\phi_u \qquad (98)$$
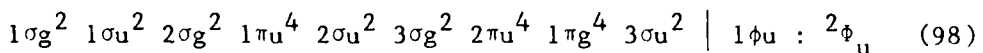
An extensive series of calculations of the possible low-lying symmetries of UO_2^+ now definitely establish this to be the ground state, but also predict a very low-lying $^2\Delta_u$ state.

A series of calculations of the low-lying electronic states of U^{+3}, U^{+4} and U^{+5} was first undertaken to determine the approximate location of the electronic states of the central ion which corresponded to f → d transitions. These results are given in Table 3 which indicate that f → d promotion in these ions lies at 327, 167 and 108 nm, respectively, for U^{+3}, U^{+4} and U^{+5}. Thus strong absorption (dipole-allowed), corresponding to central ion promotion, is predicted to occur only for wavelengths shorter than ~ 300 nm for UO_2^+, since the charge state of the uranium atom must be > + 3. A spin orbit analysis of these calculated levels yields the splittings in J-J coupling. The $^2\phi_{5/2u}$ state is the predicted ground state multiplet.

In order to establish that f → d transitions in UO_2^+ lie at these short wavelengths, a series of molecular calculations of the low-lying electronic states was undertaken. The promotion of an electron out of the $1\phi_u$ MO of UO_2^+, which is nearly purely uranium atom in composition, gives rise to the one-electron spectra shown in Table 4. The u → u intra-f-shell transitions are dipole-forbidden and correspond to the several weak absorption bands observed in solutions of UO_2^+ (Reference 83). The lowest dipole-allowed f → d transitions on the central uranium atom corresponds to the $^2\phi_u$ (^5f_u) → $^2\Delta_g$ ($6d_g$) excitation at λ ~ 300 nm. This transition lies beyond the region of efficient solar pumping of UO_2^+. Hay (Reference 84) reports a similar transition in his effective potential studies of UO_2^+, but at a somewhat shorter wavelength (~ 250 nm).

A separate molecular spectra for UO_2^+ arises from charge transfer states formed by promotion of an electron from (mainly) ligand MO's to a central uranium atom MO. Preliminary calculations (Reference 76) indicated that several of these states lie in the 300-400 nm region, and would therefore be efficiently solar pumped. A careful re-analysis of the ground $^2\phi_u$ state indicated a false convergence onto local minima in the orbital parameter space. This produced a ground state potential curve with an internuclear separation that was too large, yielding excitation energies that were correspondingly too small. Careful convergence studies and the employment of a new integration scheme now gives an equilibrium U-O bond length in UO_2^+ of 1.73 Å. This value, coupled with a fundamental ν_3 vibrational frequency of 880 cm^{-1}, is now in good agreement with Badger's rule (Reference 85) correlating bond lengths and force constants for actinide salts and oxo-ions:

$$R(U-O) \simeq 1.08 \, k^{-1/3} + 1.17 \qquad (99)$$

Using these more reliable integration methods, the low-lying charge transfer states of UO_2^+ were re-examined; their term levels are given in Table 5. These charge transfer states, some of which would exhibit very strong absorption, begin at $\sim$ 47,000 cm^{-1} $\left[^4\Pi_u\right]$, with the first strong dipole allowed transitions corresponding to the excitation $1\pi g^4 \, 1\phi u \to 1\pi g^3 \, 1\phi u^2$. These transitions lie at 53,000 $\to$ 57,000 cm^{-1}, which correspond to absorption wavelengths in the VUV, well outside of the region for efficient solar pumping. A composite potential energy curve for UO_2^+, including both central uranium atom excitation states and the low-lying ligand to central atom charge transfer states, is given in Figure 1. Our calculated assignments of the $f \to f$, $f \to d$ and charge transfer excitations among the low-lying states are given in Table 6.

This oxo-ion exhibits two different characteristic equilibrium U-O separations. They correspond to $U^{+5} (O^{-2})_2$ configurations with a short bond and to $U^{+4} (O^{-1.5})_2$ charge transfer states which exhibit a weakened U-O bond and correspondingly longer equilibrium bond length. The spin orbit analysis for UO_2^+ is presently being carried out but this analysis will not affect our conclusion that solar pumping of electronically excited states of UO_2^+ has a low efficiency.

An analysis of the LWIR emission from UO_2^+ has been carried out based on the ground $^2\phi_{5/2u}$ electronic state. These calculations should also be repre-

sentative of the LWIR emission from other low-lying electronic states since they all exhibit similar ionicities. The spectroscopic data for the $^2\phi_{5/2u}$ state, derived from our calcuated ground state potential curve, are shown in Table 7. We find a small anharmonicity in the IR active, asymmetric ν_3 vibration, similar to that found in the highly ionic UO^+ and UO molecules. Our calculated f-numbers, including fundamentals and overtones are given in Table 8 for the lowest 9 vibrational levels. We have also included the emission wavelengths for each transition. For UO_2^+, our calculated f-number for the 1-0 transition is 1.2×10^{-4} at $\lambda = 11.43~\mu$. This can be compared with a calculated f-number of 5.2×10^{-5} at $\lambda = 11.3~\mu$ for UO^+. Relatively strong LWIR is therefore predicted for UO_2^+.

4.4 UO_2.

An extensive set of calculations for the ground state of UO_2 was carried out in $D_{\infty h}$ symmetry. The ground electronic state has the dominant molecular orbital configuration:

$$^1\Sigma_g^+: \quad [1\sigma_g^2~1\sigma_u^2~2\sigma_g^2~1\pi_u^4~2\sigma_u^2~3\sigma_g^2~2\pi_u^4~1\pi_g^4~3\sigma_u^2~1\phi_u^2] \quad (100)$$
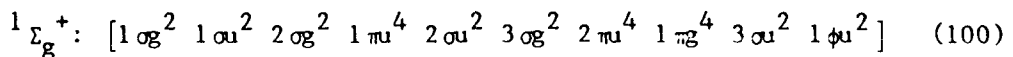
We find an equilibrium internuclear separation of 1.81 Å, a value somewhat larger than that corresponding to the various uranyl oxo-ions. At present it is uncertain whether this represents a deficiency in the calculations or whether significant back-bonding of electron charge to the central uranium atom is occurring in the gas phase UO_2 species. This would result in a lengthening of the U-O bond and a corresponding decrease in the U-O bond strength. The first excited electronic state of UO_2 corresponds to a $1\phi u \rightarrow 3\pi u$ electron promotion. This state lies at ~ 1.4 eV but we predict very weak solar pumping since the transition is not dipole allowed. The first strongly allowed transition corresponds to a $1\phi u \rightarrow 1\delta g$ electron promotion at ~ 3.4 eV. This transition lies at ~ 360 nm putting it out of the region of efficient solar pumping.

Calculations of the electronic structure and LWIR characteristics of neutral UO_2 have been undertaken. Current estimates of the LWIR properties of UO_2 are based on UO_2^+ which has an IR active ν_3 mode. We find neutral UO_2 to be a linear molecule with geometry similar to that found for UO_2^+:

	UO_2^+	UO_2
Group	$D_{\infty h}$	$D_{\infty h}$
ν_3 (cm^{-1})	880.0	776.1
x_3 (cm^{-1})	2.7	3.0
r (Å)	1.73	1.80

The characteristic f_{01} - number of UO_2 (asymmetric stretch mode) is computed to be $f_{01} = 1.1 \times 10^{-4}$ at 12.9 μ. This can be compared with our calculated values for UO_2^+ ($f_{01} = 1.2 \times 10^{-4}$ at $\lambda = 11.43$ μ) and UO^+ ($f_{01} = 5.2 \times 10^5$ at $\lambda = 11.3$ μ). The LWIR properties of UO_2 are very close to the single ionized species UO_2^+.

4.5 TiO^+.

A preliminary thermodynamic analysis of the titanium/oxygen system has been carried out. The results are given in Fig. 2 where we indicate the relative energetics of Ti/O_2 and the first and second ionization levels of this system. Several very interesting results have been obtained. First, we confirm that the associative ionization reaction:

$$Ti + O \rightarrow TiO^+ + e \tag{101}$$
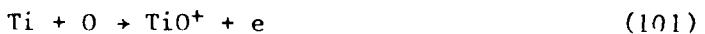
is exothermic by 0.47 eV and would be an early time (or high altitude chemistry) conversion route for $Ti \rightarrow TiO^+$. TiO^+ is stable against further oxidation by O atoms but is converted to TiO_2^+ by the reaction:

$$TiO^+ + O_2 \rightarrow TiO_2^+ + O \tag{102}$$

which is exothermic by ~ 1.6 eV. The highly stable structure of TiO_2^+ indicates that the associative ionization reaction:

$$Ti + O_2 \rightarrow TiO_2^+ + e \tag{103}$$

is exothermic by ~ 2.1 eV. Thus the chemistry of the titanium/oxygen system parallels that of the uranium/oxygen system.

An analysis of the electronic structure and spectroscopy of the TiO^+ ion has been carried out. The calculated spectroscopic data are given in Table 9. We find that the ground state of TiO^+ has $^2\Delta$ symmetry. However, the $^2\Sigma^+$ state lies < 0.5 eV in excitation and several other low-lying electronic states have been found. A surprising result of our studies is that the dipole moment function for the ground $X^2\Delta$ state of TiO^+ is a weak function of the internuclear separation near R_e. In addition, we find that the absolute value of

the dipole moment is ~ 7 debyes, a value smaller than that typically found for other metal oxides. This suggests that the bonding in TiO^+ (and TiO) is more covalent than in the nearly completely filled d-shell metals. We estimate an ionicity of approximately 73%. Our calculated oscillator strengths for LWIR in TiO^+ yields $f_{10} = 4.4 \times 10^{-6}$, a value much smaller than that found for UO^+ (5.2×10^{-5}) and for other similar metal oxides. The fundamental band is at 10.3 μ, with a very weak first overtone at 5.2 μ. The oscillator strengths for the first six vibrational levels are given in Table 10. Further studies of electronically excited states of TiO^+ are indicated to complete our LWIR analysis of this system. In addition, the stability, structure and radiative properties of TiO_2^+ will be the subject of future research.

4.6 $e + U^+$, $e + U^{++}$ DIELECTRONIC RECOMBINATION.

In addition to our calculations of the structure and radiative properties of metal/oxygen species, an analysis of the importance of dielectronic recombination processes has been initiated. Dielectronic recombination (DR) is the process by which electron capture from the continuum to a bound state is facilitated by collisional excitation of a previously bound target electron. The process can be represented by:

$$e + U^{+q} \longrightarrow [U^{+q-1}]^{**} \tag{104}$$

$$[U^{+q-1}]^{**} \longrightarrow [U^{+q-1}]^{*} + h\nu \tag{105}$$
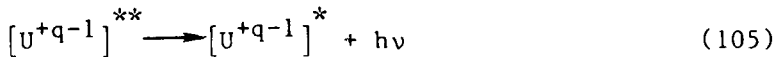
where $[U^{+q-1}]^{**}$ is a doubly excited state of the system at ionization level $(+q-1)$ and $[U^{+q-1}]^{*}$ is a stabilized excited state lying below the U^{+q-1} ionization threshold. The process is shown schematically in Figure 3. In the case of recombination unperturbed by external fields or the plasma density, the rate coefficient can be calculated as:

$$\alpha_{i,j,k}(\varepsilon) = \frac{2}{g_i} \left[\frac{\pi a_o^2}{T} \right]^{3/2} \frac{\mathcal{A}_{ji}(\varepsilon) \, A_{jk}}{\sum\limits_{i',k'} \mathcal{A}_{ji'}(\varepsilon) + A_{jk'}} \, e^{-\varepsilon_j/kT} \tag{106}$$

where $\mathcal{A}_{ji}(\varepsilon)$ is the rate of autoionization from state $|j\rangle$ into the continuum state $|i\rangle$, A_{jk} is the radiative rate from state $|j\rangle$ into the final bound state $|k\rangle$ and the sum is over all possible open channels.

An analysis of the low-lying electronic states of U^0, U^{+1} and U^{+2} has been carried out to establish a data base for examining the role of DR in uranium. The calculated energy spectra for U^0, U^{+1} and U^{+2} are given in Tables 11-13, respectively. The states examined include all one-electron promotions of U^{+q}, followed by one electron capture final configurations which correspond either to high-lying Rydberg states or bound valence excited states of the U^{+q-1} system. Tables 14 and 15 summarize the low-lying states which are important for DR of $e + U^+$ and $e + U^{++}$, respectively. There are two low-lying configurations for U^{++} which have the J-J coupled representations, $[5f_{5/2}^3 7s]$ and $[5f_{5/2}^3 6d_{3/2}]$. These two configurations are separated by only 4117 cm^{-1} and both can be formed by successively removing two electrons from the ground state neutral U^0 configuration, $[5f_{5/2}^3 7s^2 6d_{3/2}]$. Two other U^{++} representations are also possible, $[5f_{5/2}^2 7s^2]$ and $[5f_{5/2}^2 7s6d_{3/2}]$, but these states lie much higher in energy and would have negligible population, even in a 10,000 K plasma.

In the case of $e + U^+$ DR (Table 14), at least two channels are accessible for low-energy electron attachment. Since the Rydberg structure lies $\leq$ 2000 cm^{-1} from the U^+ ionization limit, several more states are open DR channels for electrons with T_e = 2000-5000 K.

The low-lying excited DR electronic states of U^{++} are shown in Table 15, relative to both the $e + U^{++}[5f_{5/2}^3 7s]$ and $e + U^{++}[5f_{5/2}^2 6d_{3/2}]$ reactant channels. These data indicate that the first open attachment channel for dielectronic recombination $e + U^{++}[5f_{5/2}^3 7s]$ occurs at $T_e \sim$ 4000 K. However, the cross-section for capture into this channel is very low since it involves a $5f_{5/2} \longrightarrow 7p_{3/2}$ promotion which has a low transition probability. The first reaction channel for DR of $e + U^{++}$ with a significant cross-section results from the allowed $7s \longrightarrow 6d_{3/2}$ transition. This channel opens for electron collision energies, $T_e \gtrsim$ 5000 K, where electron capture into a high lying Rydberg orbital can occur. However, the probability of subsequent autoionization is now competitive with radiative stabilization and the dielectronic recombination rate coefficient is of the order of 10^{-12} cm^3/sec or less.

We conclude that dielectronic recombination of e + U^{++} is a low probability process and not rate competitive with possible ion-neutral charge exchange reactions. In contrast, dielectronic recombination of e + U$^+$ has a much higher probability and may approach gas kinetic rates for $T_e \gtrsim 10^3$K. Detailed rate calculations of this process are in progress.

4.7 N + O$_2$.

As a final task under this Contract, a study of the atmospheric reactions O + N$_2$ and N + O$_2$ which yield vibrationally excited NO molecules has been initiated. The sources of NO emission in the IR are not fully understood and the detailed kinetic branching of these reactions is being studied. In particular, the role of the N[^{2}P] + O$_2$[X$^3\Sigma_g^-$] reaction in the production of vibrationally excited NO molecules is being examined. The current NORSE code assumes that all of the exothermicity of this reaction goes into vibrational excitation of the NO product molecule, with all levels being equally populated up to v = 26. In Table 16, we show the correlations connecting the N + O$_2$ reactants to NO + O product states. A schematic diagram of these correlations for C$_s$ symmetry is shown in Figures 4 and 5 for doublet and quartet states respectively. This diagram is a somewhat more complete version of that given by Donovan and Husain (Reference 86).

The adiabatic reaction surfaces arising from N[^{2}P] + O$_2$ are the following:

$$N^*[^2P] + O_2[X^3\Sigma_g^-] \longrightarrow NO_2^*[^2A'x] \qquad \longrightarrow NO^*[a^4\Pi_g] + O[^3P] + .212 \text{ eV} \qquad (107)$$

$$\longrightarrow NO_2^*[^4A'vi] \qquad \longrightarrow NO^*[a \quad _g + O \quad P] + .212 \qquad (108)$$

$$\longrightarrow NO_2^*[^2A''viii] \qquad \longrightarrow NO\,[X^2\Pi] + O^*[^1D] + 3.010 \qquad (109)$$

$$\longrightarrow NO_2^*[^4A''v] \qquad \longrightarrow NO^*[a^4\Pi_g] + O[^3P] + .212 \qquad (110)$$

$$\longrightarrow NO_2^*[^2A''ix] \qquad \longrightarrow NO\,[X^2\Pi] + O^*[^1S] + .788 \qquad (111)$$

$$\longrightarrow NO_2^*[^4A''vi] \qquad \longrightarrow NO^*[a^4\Pi_g] + O[^3P] + .212 \qquad (112)$$
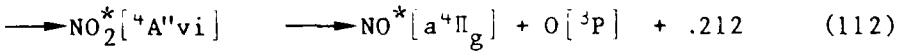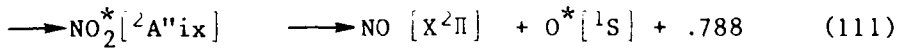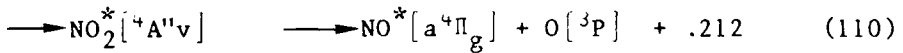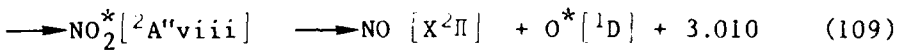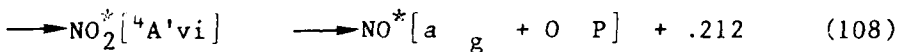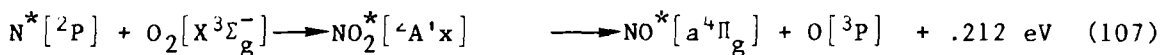
Only the third reaction [yielding NO(X$^2\Pi$) + O*(^{1}D)] is exothermic enough to yield NO with a significant degree of vibrational excitation, provided that this reaction proceeds along an adiabatic pathway. However, there is spectroscopic evidence that curve-crossing and non-adiabatic behavior does

55

occur for this system. The ground $^2A_1$ state of NO_2 must adiabatically correlate to the reactants; $N^*[^2D] + O_2[X^3\Sigma_g^-]$, whereas the first excited $^2B_1$ state correlates to ground state reactants, $N[^4S] + O_2[X^3\Sigma_g^-]$. In addition, Gilmore (Reference 87) has pointed out that NO quenching of both $O^*[^1S]$ and $O^*[^1D]$ proceeds very rapidly, further indicating curve-crossings in the doublet surfaces.

In order to clarify the branching kinetics of the $N^*[^2P] + O_2[X^3\Sigma_g^-]$ reaction, we have initiated an extensive series of calculations of the potential energy reaction surfaces for NO_2 in the following symmetries: $^2A'$, $^2A''$, $^4A'$, $^4A''$. Preliminary CI calculations were carried out in C_s symmetry assuming a frozen core of $(1a_1^2) (1b_2^2) (2a_1^2) (3a_1^2) (2b_2^2) (4a_1^2)$, which is the Hartree - Fock representation of the inner 1s and 2s electrons. Unfortunately, the characteristic charge density corresponding to this core representation differs significantly for different spin and spatial couplings of N + O_2. The characteristic charge of the $(4a_1^2)$ pair, for example, differs in calculations in $^2A'$ symmetry as compared with $^2A''$ or $^4A'$ symmetry. Thus only a frozen inner shell (1s electrons) appears to be possible for this system. This smaller frozen core representation results in a great increase in the CI size, from 2-3000 to 20-30000. The calculations must therefore be carried out on a CRAY computer and the necessary code modifications for running this problem on the DNA access machines at LANL are in progress. Our calculations will be carried out in C_s symmetry since we need to simultaneously examine the N + O_2 reaction path on twelve surfaces in $^2A'$ and $^2A''$ symmetry and on six surfaces in $^4A'$ and $^4A''$ symmetry.

SECTION 5

RECOMMENDATIONS

Previous studies of the electronic structure and energy levels of the uranium/oxygen system have been undertaken by UTRC and reported in DNA-TR-82-159 (Reference 75), DNA-TR-85-156 (Reference 76) and the present technical report for Contract DNA001-85-C-0120. In these studies the focus was on estimating the LWIR radiation characteristics and the efficiency of solar pumping of the allowed electronic transitions in this system which fall in the visible wavelength region. An examination of the thermodynamics and kinetics of the uranium/oxygen system shows that U^+ and UO^+ are terminal ions, and therefore potentially important radiators at high altitudes, whereas UO_2^+ is more important at low altitudes where there is significant O_2 concentration. Our preliminary studies also indicated that TiO^+ is not an important LWIR radiator but that TiO_2^+ may be an important ion at low altitudes. Further studies of the uranium/oxygen system are outlined below. In addition, suggested studies of dielectronic recombination and kinetic branching in atmospheric reactions producing radiating NO molecules are described.

5.1 URANIUM/OXYGEN.

The calculations of the electronic structure of the uranium oxide ions have been performed with neglect of the spin-orbit interaction term, optimizing the relativistic density functional SCF wavefunctions for the particular ion. Spin-orbit interaction is then introduced as a perturbation through configurational mixing. This same approach has been used by Krauss and Stevens (Reference 78), with a full ab initio treatment of the valence electrons, using ℓ-dependent relativistic effective core potentials. Either approach allows for polarization and charge transfer from the ligand oxygen atoms to the central uranium ion.

A different approach for rare earth metal oxides has been described by Dulick (Reference 81) which is based on a crystal field model. Application of this method to the UO and UO^+ ground states (Reference 89) yields a significantly different energy ordering for the Ω coupled states than is found in the full molecular treatments of the systems described above. The application of the crystal field model to lanthanide monoxides, however, appears to yield the

57

known experimental electronic assignments (Reference 90). An examination of the composition of the predicted Ω states for UO^+, based on this crystal field model, indicates a significant mixing of electronic states of the uranium ion of small ℓ-value. These effects are not found in the molecular treatments, whose compositions are dominated by the tightly coupled 5f states. Further studies of these differences in approach are indicated; however, since all methods are either based on or predict a large ionic character in the UO^+ and UO_2^+ ions, our conclusion of strong LWIR emission should not be altered. The crystal field model has not been utilized for describing electronic transitions or the absorption/emission characteristics in either the IR or visible wavelength regions.

Our suggested studies include the further examination of low-lying electronic states in UO^+ and UO_2^+. These studies will primarily cover the IR, visible and UV excitation wavelengths ($< \sim 5$ eV) in order to more accurately define the radiation emission strengths. A new density functional computer code, that is being developed in collaboration with Professor F. E. Harris (U. of Utah), will be utilized to carry out these suggested studies. This new code yields a more accurate representation of the electron density in the valence region between atomic centers. This region has previously been described by a constant (muffin-tin) potential which can lead to inaccuracies in describing polarization effects. We feel that this new code would also permit a more critical evaluation of the crystal field model, as applied to the uranium/oxygen system.

Our increase in the data base for the uranium/oxygen system will include radiation f-numbers, characteristic absorption/emission wavelengths and calculated density of states for U^{+n}, UO^{+n}, UO_2^{+n} ($n = 0,1,2$). In a smaller effort, the radiation properties of TiO^+ and TiO_2^+ should be more accurately defined.

5.2 DIELECTRONIC RECOMBINATION.

In addition to our suggested calculations of the structure and radiative properties of uranium/oxygen species, further analysis of the importance of dielectronic recombination processes should be carried out. A preliminary study of the important dissociative recombination states of U°, U^+ and U^{++} has been described above under Section 4. Several highly excited configurations for U° have been identified which indicate that $e + U^+$ may be an important

58

charge neutralization process, but a more extensive study is required to determine the density of states accessible to dielectronic recombination under conditions up to perhaps 5000°K.

A corresponding DR process is possible for $e + UO^+$. At the present time, only the optically connected excited states of UO^+ have been studied. The ground molecular orbital configuration for UO^+ is:

$$^4I\left[1\sigma^2\ 2\sigma^2\ 3\sigma^2\ 4\sigma^2\ 1\pi^4\ 2\pi^4\ \vdots\ 3\pi\ 1\phi\ 1\delta\right] \qquad (115)$$
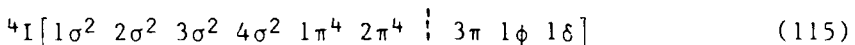
where the last three molecular orbitals are nearly pure f-orbitals centered on uranium. Excitation processes that need to be examined, all in a molecular framework, are: $f^2 \rightarrow d^2$, $f^2 \rightarrow s^2$, $f^2 \rightarrow sd$ $f^2 \rightarrow p^2$, $f^2 \rightarrow sp$ and $f^2 \rightarrow pd$. Additional excitations from the core 2π level will be examined but it is expected that these levels are too tightly bound for the electron energy range of interest.

These studies of dielectronic recombination contribute to our understanding of the kinetics of charge neutralization following nuclear bursts. In particular, the role of dielectronic recombination as a mechanism for removal of electrons is uncertain at present and, if found to be important, must be included in the chemistry kinetics in the NORSE code.

5.3 NO/NO$^+$ FORMATION.

Under this Contract, DNA001-85-C-0120, a study of the atmospheric reactions $O + N_2$ and $N + O_2$ which yield vibrationally excited NO molecules was initiated. This study was in response to the requirement defined by Gilmore (Reference 87) for a more accurate analysis of the $N\left[^2D\right] + O_2$ and $N\left[^2P\right] + O_2$ reactions which are modeled in the NORSE calculation of NO chemiluminescence. Since the $N\left[^2P\right] + O_2$ reaction can yield $N\left[^2D\right] + O_2$ as products, as well as vibrationally excited NO, there is a large uncertainty in the kinetic branching at the present time. If vibrationally hot NO is strongly favored as the product channel, high IR emission at 9 μm and 4.5 μm is predicted. We suggest a study of these reactions, including all energetically allowed product channels. Detailed quantum mechanical calculations of twelve reaction surfaces are required, necessitating the use of a CRAY-class computer.

In a closely related problem, a strong radiator in the IR following a nuclear burst is vibrationally excited NO$^+$, with emission near 4.3 μm. An

examination of the ion-molecule reaction surface for $0 + N_2^+$, $O_2^+ + N$, and $O^+ + N_2$ should be carried out to establish the overall product correlations for this system. If required, detailed quantum mechanical studies of the pertinent reaction surfaces should be examined. A similar study of the $O^+ + N_2 \rightarrow NO^+ + N$ reaction has been previously carried out for DNA by UTRC under AFGL Contract F19628-80-C-0209 (Reference 91). All of these studies of atmospheric molecules have the objective of increasing the fundamental data base of the reaction kinetics in order to provide useful input for chemilumi-nescence modeling in the various atmospheric codes.
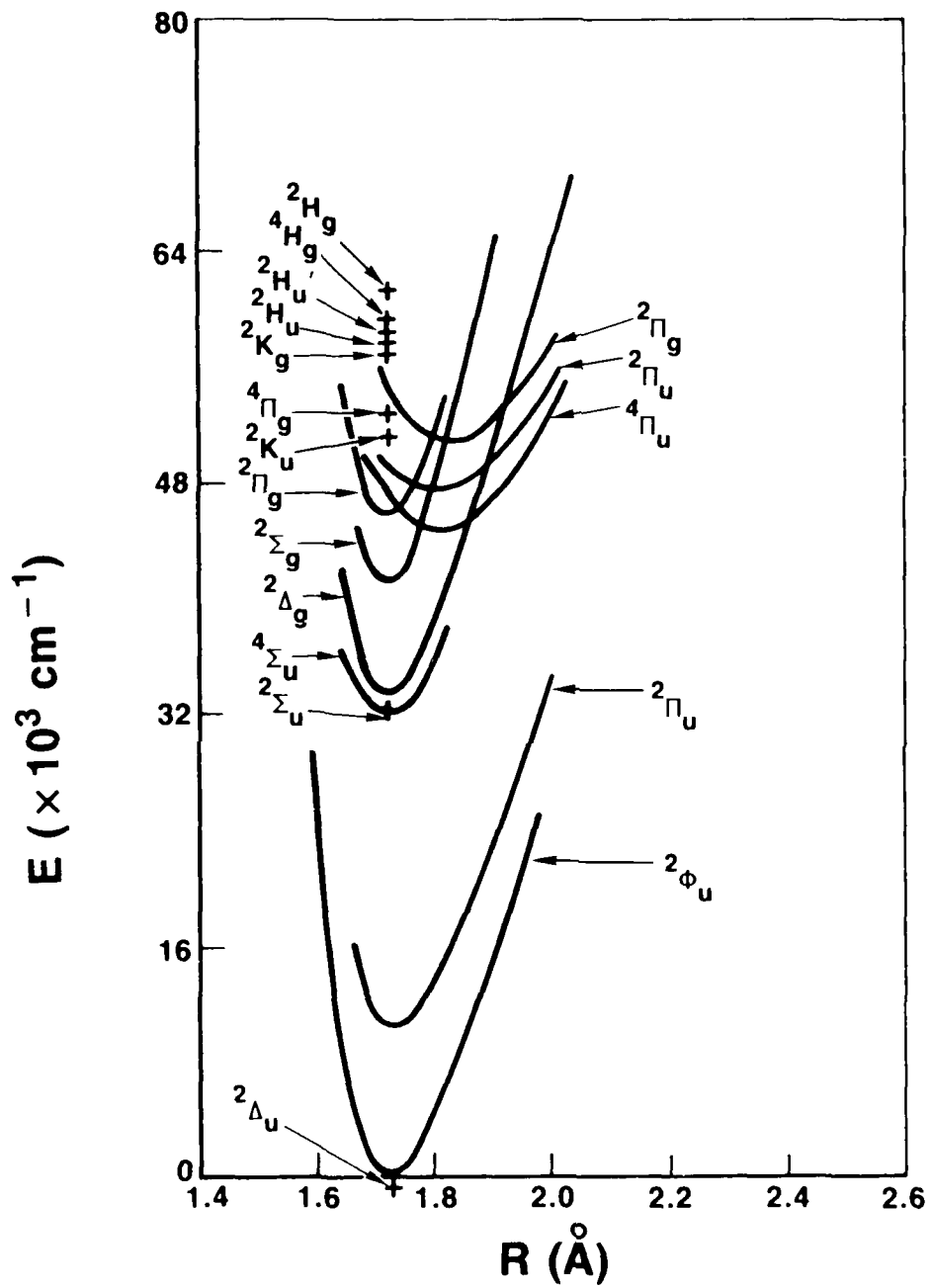
Figure 1. Potential energy curves for UO_2^+.
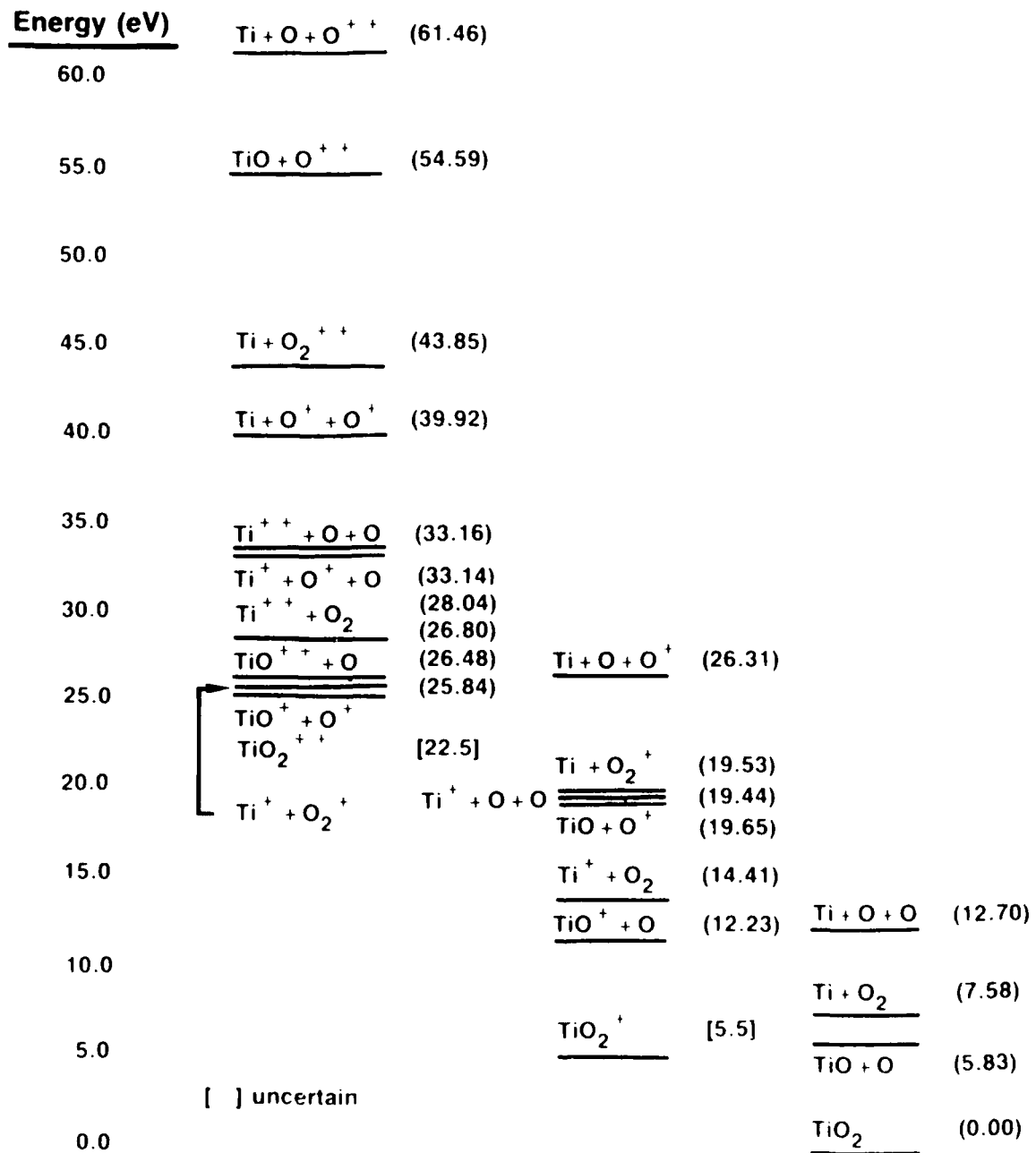
Figure 2. Thermodynamic stability of titanium/oxygen species.
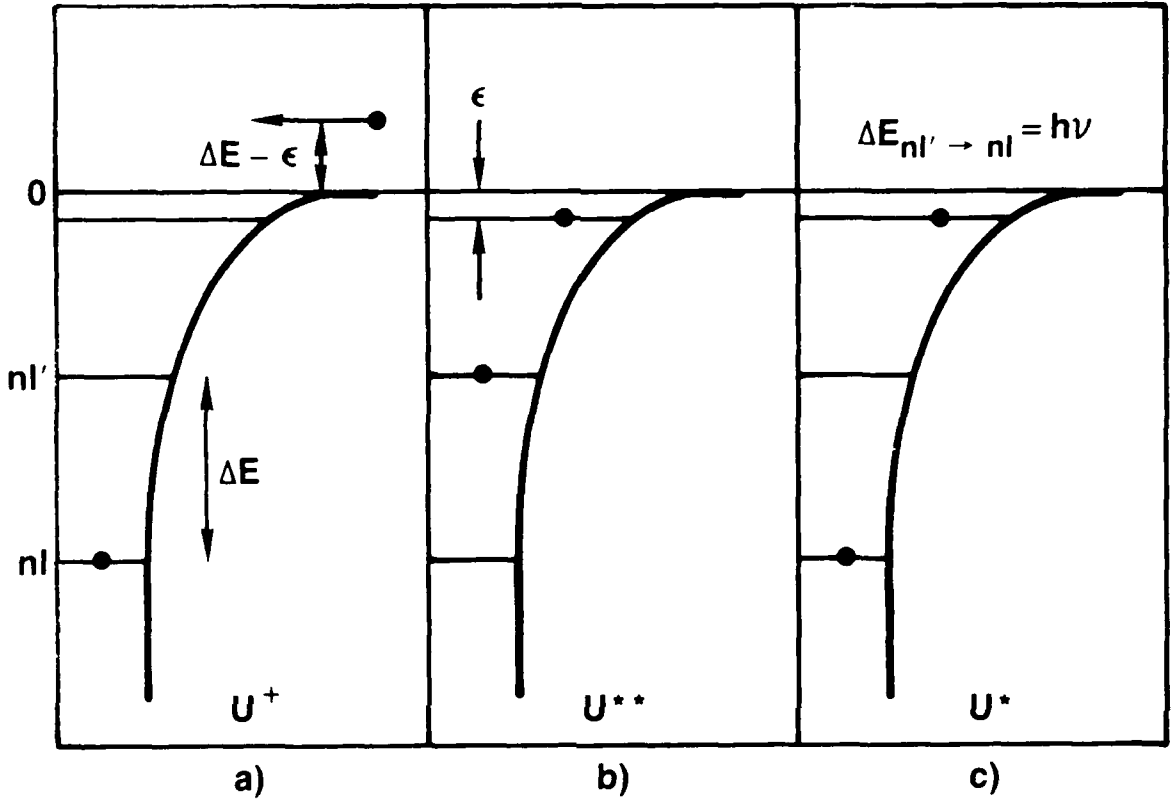
a) Incoming electron has energy less than $E_{nl'} - E_{nl}$.

b) Incoming electron + KE in Coulomb field excites an electron from nl ⟶ nl' and incident electron is trapped in a highly excited state.

c) Doubly excited state radiates (nl' ⟶ nl) resulting in a stable excited state lying below the ionization threshold.

Figure 3. Dielectronic recombination.
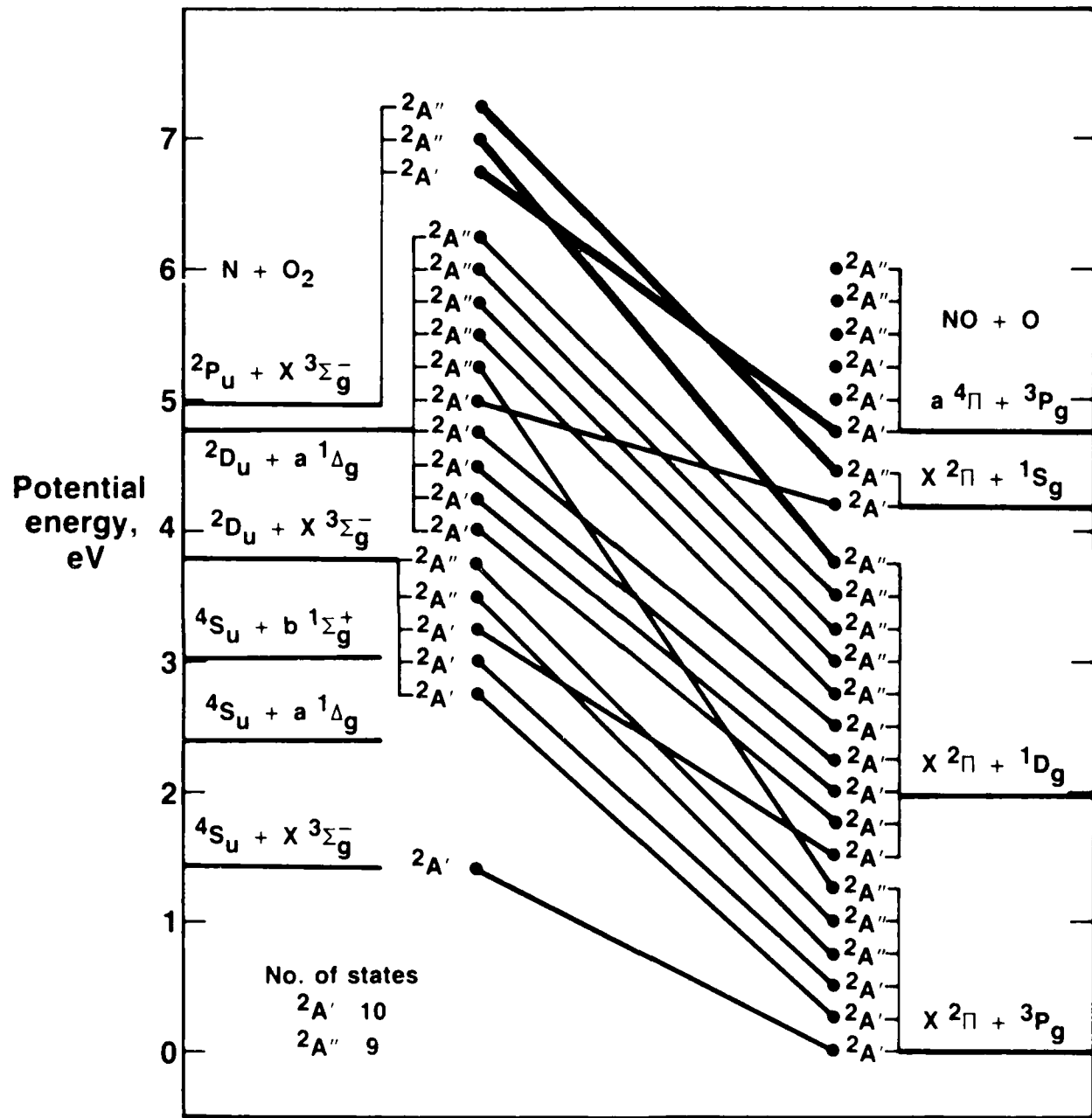
Figure 4. Molecular correlation diagram for low-lying states of NO_2 in C_s symmetry. (doublet states)
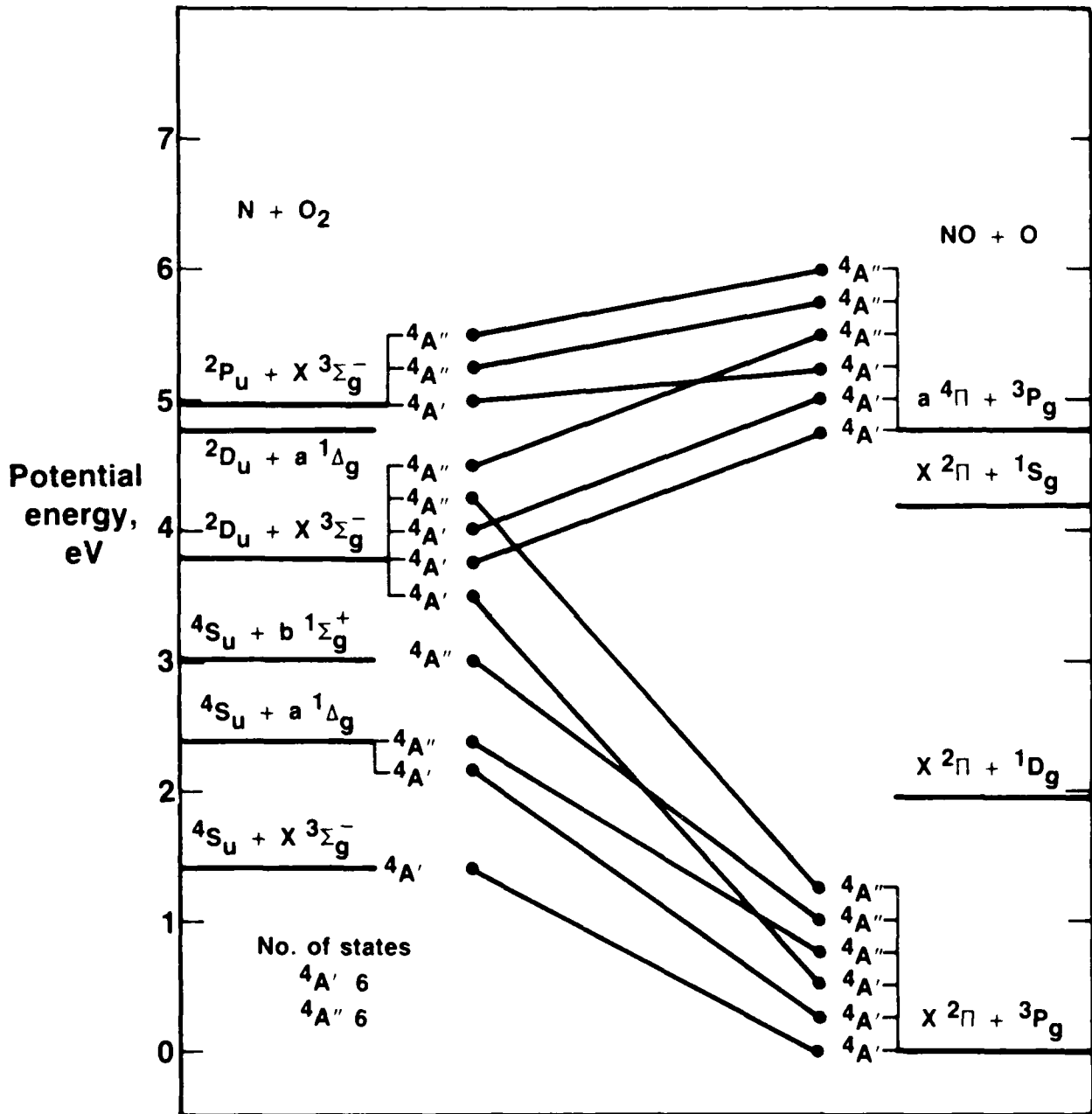
Figure 5. Molecular correlation diagram for low-lying states of NO_2 in C_s symmetry. (quartet states)

Table 1. Calculated spectroscopic data for UO/UO$^+$.

	UO [^{5}I]	UO$^+$ [^{4}I]
$\omega_e(cm^{-1})$:	820 (matrix)	949 (SCF)
	836 (scaled from ThO)	935 (MCSCF)
	863 (SCF)*	925 (MCSCF: $\Omega = 9/2$)
	845 (MCSCF)*	980 (RDF-UTRC)
	859 (RDF-UTRC)	
$\omega_e X_e(cm^{-1})$:	2.7 (H-H potential)	2.7 (H-H potential)
	i2.0 (^{3}I excited state)	
$R_e(\text{Å})$:	1.84 (matrix)	1.83 (SCF)
	1.838 (Heaven and Nicolai)**	
	1.88 (SCF)	1.84 (MCSCF)
	1.84 (MCSCF-Krauss)	1.84 (RDF-UTRC)
	1.89 (RDF-UTRC)	
	1.838 (Kaledin, et al)***	

----

*SCF and MCSCF results, see Reference 78.
**See Reference 79.
***See Reference 80.

66

Table 2. 5f spin-orbit parameters for U^{+n} ions.

Configuration	ζ (cm^{-1}) LASL (Wood, Boring)[*]	RDF
U^{+5} (5f)	2442	2455
U^{+4} (5f^2)	2212	2220
U^{+3} (5f^3)	1977	1983

$$\zeta = \frac{2}{2\ell+1} \left(\epsilon^k - \epsilon^{k^*} \right); \quad k^* = \ell \text{ for } j - 1/2$$
$$k = -(\ell + 1) \text{ for } j + 1/2$$

[*]Ref. 57

Table 3. Calculated energy spectra for U^{+3}, U^{+4}, U^{+5}

	Configuration	E (cm^{-1})
U^{+3}	$5f^3{}_{5/2}$	0.
(ζ_{5f} = 1983 cm^{-1})	$5f^2{}_{5/2}\, 5f_{7/2}$	6938.
(ζ_{6d} = 2873 cm^{-1})	$5f_{5/2}\, 5f^2{}_{7/2}$	13898.
	$5f^3{}_{7/2}$	28890.
	$5f^2{}_{5/2}6d_{3/2}$	30592.
	$5f^2{}_{5/2}6d_{5/2}$	37774.
	$5f_{5/2}5f_{7/2}6d_{3/2}$	38166.
	$5f_{5/2}5f_{7/2}6d_{5/2}$	45342.
	$5f^2{}_{7/2}6d_{3/2}$	45754.
	$5f^2{}_{7/2}6d_{5/2}$	52938.
U^{+4}		
(ζ_{5f} = 2220 cm^{-1})	$5f^2{}_{5/2}$	0.
(ζ_{6d} = 3353 cm^{-1})	$5f_{5/2}5f_{7/2}$	7770.
	$5f^2{}_{7/2}$	15570.
	$5f_{5/2}6d_{3/2}$	60032.
	$5f_{5/2}6d_{5/2}$	68410.
	$5f_{7/2}6d_{3/2}$	68912.
	$5f_{7/2}6d_{5/2}$	77302.
U^{+5}		
(ζ_{5f} = 2455 cm^{-1})	$5f_{5/2}$	0.
(ζ_{6d} = 4268 cm^{-1})	$5f_{7/2}$	8592.
	$6d_{3/2}$	92921.
	$6d_{5/2}$	103590.

Table 4. Term levels for central atom (one-electron) excitation of UO_2^+.

Molecular Orbital	Symmetry	Te (cm^{-1})
$1\phi u$	$^2\Phi_u$	0.
$1\delta u$	$^2\Delta_u$	-362.*
$3\pi u$	$^2\Pi_u$	10118.
$4\sigma g$	$^2\Sigma_u^+$	32250.
$1\delta g$	$^2\Delta_g$	33163.
$1\sigma g$	$^2\Sigma_g$	40976.
$2\pi g$	$^2\Pi_g$	45695.

---

*Although the center-of-gravity of the $1\delta u$ state lies lower than $1\phi u$, spin-orbit splitting causes the $^2\Phi_{5/2u}$ state to become the ground state, in agreement with previous studies of this system (Reference 83).

Table 5. Term levels for charge transfer states of UO_2^+.

Molecular Orbital			Symmetry	Te (cm^{-1})
$2\pi_u^4$	$1\pi g^4$	$1\phi u$	$^2\Phi_u$	0.
$2\pi u^3$	$1\pi g^4$	$1\phi u^2$	$^4\Pi_u$	47341.
$2\pi u^3$	$1\pi g^4$	$1\phi u^2$	$^2\Pi_u$	49327.
$2\pi u^3$	$1\pi g^4$	$1\phi u^2$	^2K_u	51346.
$2\pi u^4$	$1\pi g^3$	$1\phi u^2$	$^4\Pi_g$	53080.
$2\pi u^4$	$1\pi g^3$	$1\phi u^2$	$^2\Pi_g$	55132.
$2\pi u^4$	$1\pi g^3$	$1\phi u^2$	^2K_g	56943.
$2\pi u^3$	$1\pi g^4$	$1\phi u \ 3\pi u$	^2H_u	58885.
$2\pi u^4$	$1\pi g^3$	$1\phi u \ 3\pi u$	^4H_g	59576.
$2\pi u^4$	$1\pi g^3$	$1\phi u \ 3\pi u$	^2H_g	61365.

Table 6. Calculated assignments of electronic transitions in UO_2^+.

Transition	Wavelength	Strength
$^2\Phi_{5/2u} \rightarrow {}^2\Delta_{3/2u}$	$> 5\mu$ (calc)	Weak ($u \rightarrow u$)
$^2\Phi_{5/2u} \rightarrow {}^2\Delta_{5/2u}$	$1.5 - 1.6\mu$ (calc)	Weak ($u \rightarrow u$)
$^2\Phi_{5/2u} \rightarrow {}^2\Phi_{7/2u}$	1.45μ (calc)	Weak ($u \rightarrow u$)
	$\sim 1.5\mu$ (exp)	
$^2\Phi_{5/2u} \rightarrow {}^2\Pi_{3/2u}$	0.84μ (calc)	Weak ($u \rightarrow u$)
	$\sim 0.9\mu$ (exp)	
$^2\Phi_{5/2u} \rightarrow {}^2\Delta_{3/2g}$ ($f \rightarrow d$)	0.30μ (calc)	Moderately Strong ($u \rightarrow g$)
$^2\Phi_{5/2u} \rightarrow {}^2\Pi_{3/2g}$	0.18μ (calc)	Strong ($u \rightarrow g$)
$(1\pi_g^4\, 1\phi_u \rightarrow 1\pi_g^3\, 1\phi_u^2)$		
$^2\Phi_{5/2} \rightarrow {}^4H_{5/2g}$	0.16μ (calc)	Very Strong ($u \rightarrow g$)
$(1\pi_g^4\, 1\phi_u \rightarrow 1\pi_g^3\, 1\phi_u 3\pi_u)$		

Table 7. Calculated spectroscopic data for UO_2^+.

ω_3 (cm^{-1})	885.4
x_{33} (cm^{-1})	-2.7
r_e (Å)	1.73
D_e (cm^{-1})	62100. (exp)

Table 8. Calculated oscillator strengths ($f_{v',v''}$) for the vibrational transitions of UO_2^+.

v'/v''	0	1	2	3	4	5	6	7	8
0	–	–	–	–	–	–	–	–	–
1	* 1.17-04 ** 11.43	–	–	–	–	–	–	–	–
2	3.58-07 5.73	2.32-04 11.50	–	–	–	–	–	–	–
3	2.20-09 3.83	1.07-06 5.77	3.47-04 11.57	–	–	–	–	–	–
4	2.04-11 2.88	8.89-09 3.86	2.14-06 5.81	4.62-04 11.65	–	–	–	–	–
5	3.11-13 2.31	1.03-10 2.90	2.19-08 3.88	3.56-06 5.84	5.75-04 11.72	–	–	–	–
6	7.34-15 1.93	8.30-13 2.33	2.83-10 2.92	4.39-08 3.91	5.34-06 5.88	6.88-04 11.79	–	–	–
7	6.43-15 1.66	1.66-14 1.95	4.32-12 2.34	6.67-10 2.94	7.73-08 3.93	7.48-06 5.92	8.00-04 11.87	–	–
8	1.28-14 1.46	4.52-19 1.67	2.35-14 1.96	1.22-11 2.36	1.41-09 2.96	1.23-07 3.96	9.95-06 5.95	9.12-04 11.95	–
9	1.42-17 1.30	7.34-15 1.47	8.49-17 1.69	5.37-13 1.97	2.53-11 2.37	2.48-09 2.98	1.85-07 3.98	1.28-05 5.99	1.02-03 12.02

* oscillator strength
** wavelength, microns

83

Table 9. Calculated spectroscopic data and dipole moment for $TiO^+[X^2\Delta]$.

ω_e	983.1 cm^{-1}	R_e	1.59 Å
$\omega_e X_e$	4.5 cm^{-1}	B_e	0.5568 cm^{-1}
α_e	0.00348 cm^{-1}	D_e	5.8890 cm^{-1}

$R(Å)$	$\mu(debye)$
1.45	6.54
1.50	7.02
1.55	7.41
1.60	7.15
1.65	6.98

Table 10. Calculated oscillator strengths ($f_{v'v''}$) for the vibrational transitions of TiO^+.

v'/v''	0	1	2	3	4	5
0	–	–	–	–	–	–
	–	–	–	–	–	–
1	*4.40-06	–	–	–	–	–
	**10.26	–	–	–	–	–
2	1.87-08	9.28-06	–	–	–	–
	5.16	10.35	–	–	–	–
3	7.46-11	5.29-08	1.47-05	–	–	–
	3.45	5.20	10.46	–	–	–
4	2.96-11	1.83-10	1.03-07	2.06-05	–	–
	2.60	3.49	5.25	10.56	–	–
5	2.60-11	5.63-11	3.67-10	1.76-07	2.72-05	–
	2.09	2.63	3.52	5.30	10.66	–
6	2.03-13	6.42-11	2.56-11	3.47-10	2.73-07	3.45-05
	1.75	2.11	2.65	3.55	5.35	10.76

*Oscillator strength
**Wavelength, microns

Table 11. Calculated energy spectra for neutral uranium, U°.

$$\left(\zeta_{5f} = 1832 \ \text{cm}^{-1}; \ \ \zeta_{6d} = 1435 \ \text{cm}^{-1} \right)$$

Atomic Configuration	Energy (cm^{-1})	Atomic Configuration	Energy (cm^{-1})
$5f_{5/2}^3 7s^2 6d_{3/2}$	0.	$5f_{7/2}^3 7s^2 7p_{1/2}$	28782.
$5f_{5/2}^3 7s^2 6d_{5/2}$	3588.	$5f_{5/2} 5f_{7/2}^2 7s 6d_{3/2} 6d_{5/2}$	31530.
$5f_{5/2}^2 5f_{7/2} 7s^2 6d_{3/2}$	6411.	$5f_{5/2}^3 7s 7p_{1/2}^2$	32337.
$5f_{5/2}^3 7s^2 7p_{1/2}$	8691.	$5f_{7/2}^3 7s^2 7p_{3/2}$	34146.
$5f_{5/2}^2 5f_{7/2} 7s^2 6d_{5/2}$	10190.	$5f_{7/2}^3 7s 6d_{3/2}^2$	34578.
$5f_{5/2}^2 7s^2 6d_{3/2}^2$	12815.	$5f_{5/2} 5f_{7/2}^2 7s 6d_{5/2}^2$	34857.
$5f_{5/2} 5f_{7/2}^2 7s^2 6d_{3/2}$	12982.	$5f_{7/2}^3 7s 6d_{3/2} 6d_{5/2}$	38004.
$5f_{5/2}^3 7s^2 7p_{3/2}$	14154.	$5f_{5/2}^2 5f_{7/2} 7s 7p_{1/2}^2$	38957.
$5f_{5/2}^3 7s 6d_{3/2}^2$	14957.	$5f_{7/2}^3 7s 6d_{5/2}^2$	41553.
$5f_{5/2}^2 5f_{7/2} 7s^2 7p_{1/2}$	15275.	$5f_{5/2}^3 6d_{3/2} 7p_{1/2}^2$	42791.
$5f_{5/2} 5f_{7/2}^2 7s^2 6d_{5/2}$	16779.	$5f_{5/2}^3 7s 7p_{3/2}^2$	44527.
$5f_{5/2}^3 7s 6d_{3/2} 6d_{5/2}$	18278.	$5f_{5/2} 5f_{7/2}^2 7s 7p_{1/2}^2$	45679.
$5f_{7/2}^3 7s^2 6d_{3/2}$	19606.	$5f_{5/2}^3 6d_{5/2} 7p_{1/2}^2$	47082.
$5f_{5/2} 5f_{7/2} 7s^2 6d_{3/2}^2$	19988.	$5f_{5/2}^2 5f_{7/2} 6d_{3/2} 7p_{1/2}^2$	49432.
$5f_{5/2}^2 5f_{7/2} 7s^2 7p_{3/2}$	20718.	$5f_{5/2}^2 5f_{7/2} 7s 7p_{3/2}^2$	51368.
$5f_{5/2}^2 5f_{7/2} 7s 6d_{3/2}^2$	21416.	$5f_{7/2}^3 7s 7p_{1/2}^2$	52397.
$5f_{5/2}^3 7s 6d_{5/2}^2$	22000.	$5f_{5/2}^2 5f_{7/2} 6d_{5/2} 7p_{1/2}^2$	53738.
$5f_{5/2} 5f_{7/2}^2 7s^2 7p_{1/2}$	22191.	$5f_{5/2} 5f_{7/2}^2 6d_{3/2} 7p_{1/2}^2$	56001.
$5f_{7/2}^3 7s^2 6d_{5/2}$	23343.	$5f_{5/2} 5f_{7/2}^2 7s 7p_{3/2}^2$	58128.
$5f_{5/2}^2 5f_{7/2} 7s 6d_{3/2} 6d_{5/2}$	24882.	$5f_{5/2} 5f_{7/2}^2 6d_{5/2} 7p_{1/2}^2$	60347.
$5f_{7/2}^2 7s^2 6d_{3/2}^2$	27441.	$5f_{7/2}^3 6d_{3/2} 7p_{1/2}^2$	62667.
$5f_{5/2} 5f_{7/2}^2 7s^2 7p_{3/2}$	27485.	$5f_{7/2}^3 7s 7p_{3/2}^2$	64964.
$5f_{5/2} 5f_{7/2}^2 7s 6d_{3/2}^2$	28110.	$5f_{7/2}^3 6d_{5/2} 7p_{1/2}^2$	67212.
$5f_{5/2}^2 5f_{7/2} 7s 6d_{5/2}^2$	28216.		

Table 12. Calculated energy spectra for the uranium positive ion, U⁺.

$$(\zeta_{5f} = 1840 \text{ cm}^{-1}; \ \zeta_{6d} = 1793 \text{ cm}^{-1})$$

Atomic Configuration	Energy (cm⁻¹)	Atomic Configuration	Energy (cm⁻¹)
$5f_{5/2}^3 7s^2$	0.	$5f_{5/2}^3 6d_{5/2} 7p_{1/2}$	39868.
$5f_{5/2}^2 5f_{7/2} 7s^2$	6439.	$5f_{5/2}^2 5f_{7/2} 6d_{3/2} 7p_{1/2}$	41781.
$5f_{5/2}^3 7s 6d_{3/2}$	9589.	$5f_{5/2}^2 5f_{7/2} 7s 7p_{5/2}$	41909.
$5f_{5/2}^3 7s 6d_{5/2}$	14071.	$5f_{5/2}^3 6d_{3/2} 7p_{3/2}$	42690.
$5f_{5/2}^2 5f_{7/2} 7s 6d_{3/2}$	16151.	$5f_{5/2}^2 6d_{3/2} 6d_{5/2}^2$	43397.
$5f_{5/2}^2 7s^2 6d_{3/2}$	19924.	$5f_{5/2}^2 7s^2 7p_{1/2}$	47345.
$5f_{5/2}^2 5f_{7/2} 7s 6d_{5/2}$	20668.	$5f_{5/2}^3 6d_{5/2} 7p_{3/2}$	47415.
$5f_{5/2}^2 5f_{7/2}^2 7s$	21133.	$5f_{5/2}^2 7s 6d_{3/2} 7p_{1/2}$	48506.
$5f_{5/2}^3 6d_{3/2}^2$	21302.	$5f_{5/2}^2 5f_{7/2} 6d_{3/2} 7p_{3/2}$	49276.
$5f_{5/2}^3 6d_{3/2} 6d_{5/2}$	25424.	$5f_{5/2}^2 7s 6d_{3/2} 7p_{1/2}$	52645.
$5f_{5/2}^2 7s 6d_{3/2}^2$	25461.	$5f_{5/2}^2 7s 6d_{5/2} 7p_{1/2}$	54351.
$5f_{5/2}^2 7s^2 6d_{5/2}$	25582.	$5f_{5/2}^3 7p_{1/2}^2$	54553.
$5f_{5/2}^3 7s 7p_{1/2}$	26690.	$5f_{5/2}^2 7s^2 7p_{3/2}$	57178.
$5f_{5/2}^2 5f_{7/2} 6d_{3/2}^2$	27788.	$5f_{5/2}^2 7s 6d_{3/2} 7p_{3/2}$	57408.
$5f_{5/2}^3 6d_{5/2}^2$	29655.	$5f_{5/2}^2 6d_{3/2} 6d_{5/2} 7p_{1/2}$	58095.
$5f_{5/2}^2 7s 6d_{3/2} 6d_{5/2}$	30689.	$5f_{5/2}^2 6d_{3/2}^2 7p_{3/2}$	60825.
$5f_{5/2}^2 5f_{7/2} 6d_{3/2} 6d_{5/2}$	31962.	$5f_{5/2}^3 7p_{1/2} 7p_{3/2}$	63277.
$5f_{5/2}^2 5f_{7/2} 7s 7p_{1/2}$	33422.	$5f_{5/2}^2 7s 6d_{5/2} 7p_{3/2}$	63351.
$5f_{5/2}^2 6d_{3/2}^3$	33663.	$5f_{5/2}^2 6d_{3/2} 6d_{5/2} 7p_{3/2}$	66356.
$5f_{5/2}^3 6d_{3/2} 7p_{1/2}$	35050.	$5f_{5/2}^3 7p_{3/2}^2$	72295.
$5f_{5/2}^3 7s 7p_{3/2}$	35142.	$5f_{5/2}^2 6d_{3/2} 7p_{1/2}^2$	77734.
$5f_{5/2}^2 5f_{7/2}^2 6d_{3/2}$	35570.	$5f_{5/2}^2 7s 7p_{1/2}^2$	78212.
$5f_{5/2}^2 7s 6d_{5/2}^2$	35976.	$5f_{5/2}^2 6d_{3/2} 7p_{1/2} 7p_{3/2}$	87191.
$5f_{5/2}^2 6d_{3/2}^2 6d_{5/2}$	38568.	$5f_{5/2}^2 7s 7p_{1/2} 7p_{3/2}$	88457.
		$5f_{5/2}^2 6d_{3/2} 7p_{3/2}^2$	96804.
		$5f_{5/2}^2 7s 7p_{3/2}^2$	99132.

Table 13. Calculated energy spectra for the uranium positive ion, U^{++}.

$$\left(\zeta_{5f} = 1932 \text{ cm}^{-1}; \ \left(\zeta_{6d} = 2091 \text{ cm}^{-1}\right)\right.$$

Atomic Configuration	Energy (cm^{-1})
$5f^3_{5/2}7s$	0.
$5f^3_{5/2}6d_{3/2}$	4117.
$5f^2_{5/2}5f_{7/2}7s$	6762.
$5f^3_{5/2}6d_{5/2}$	9345.
$5f^2_{5/2}5f_{7/2}6d_{3/2}$	10846.
$5f^2_{5/2}5f_{7/2}6d_{5/2}$	16070.
$5f^2_{5/2}7s6d_{3/2}$	24660.
$5f^2_{5/2}6d^2_{3/2}$	24722.
$5f^2_{5/2}7s^2$	27632.
$5f^2_{5/2}6d_{3/2}6d_{5/2}$	30625.
$5f^2_{5/2}7s6d_{5/2}$	30979.
$5f^3_{5/2}7p_{1/2}$	31198.
$5f^2_{5/2}6d^2_{5/2}$	36597.
$5f^2_{5/2}5f_{7/2}7p_{1/2}$	38057.
$5f^3_{5/2}7p_{3/2}$	42236.
$5f^2_{5/2}5f_{7/2}7p_{3/2}$	49092.
$5f^2_{5/2}6d_{3/2}7p_{1/2}$	57535.
$5f^2_{5/2}7s7p_{1/2}$	61600.
$5f^2_{5/2}6d_{5/2}7p_{1/2}$	63990.
$5f^2_{5/2}6d_{3/2}7p_{3/2}$	69400.
$5f^2_{5/2}7s7p_{3/2}$	74336.
$5f^2_{5/2}6d_{5/2}7p_{3/2}$	75956.
$5f^2_{5/2}7p^2_{1/2}$	96294.
$5f^2_{5/2}7p_{1/2}7p_{3/2}$	109336.
$5f^2_{5/2}7p^2_{3/2}$	122544.

Table 14. Energetics of dielectronic recombination of $e + U^+$.

$e + U^+$	ε (cm^{-1})	U^*	ε (cm^{-1})
$e + [5f^3_{5/2}7s^2]$	0.	$[5f^3_{5/2}7s7p_{1/2}7p_{3/2}]$	$\sim 0.$
		$[5f^2_{5/2}7s^27p_{3/2}6d_{5/2}]$	116.
		$[5f^3_{5/2}7s7p^2_{3/2}]$	6154.
		$[5f^3_{5/2}7s6d_{3/2}n\ell]$	$9589-E_{n\ell}$
		$[5f^3_{5/2}7s6d_{5/2}n\ell]$	$14071-E_{n\ell}$
		$[5f^2_{5/2}7s^26d_{3/2}n\ell]$	$19924-E_{n\ell}$

Table 15. Energetics of dielectronic recombination of $e + U^{++}$.

$e + U^+$	ε (cm^{-1})	$[U^+]^*$	ε (cm^{-1})
$e + [5f^3_{5/2}7s]$	0.	$[5f^2_{5/2}7s7p^2_{3/2}]$	$271\,i.$
		$[5f^3_{5/2}6d_{3/2}n\ell]$	$4117.-E_{n\ell}$
		$[5f^3_{5/2}6d_{5/2}n\ell]$	$9345.-E_{n\ell}$
		$[5f^2_{5/2}7s6d_{3/2}n\ell]$	$24660.-E_{n\ell}$
		$[5f^2_{5/2}6d^2_{3/2}n\ell]$	$24722.-E_{n\ell}$
$e + [5f^3_{5/2}6d_{3/2}]$	4117.	$[5f^3_{5/2}6d_{5/2}n\ell]$	$5228.-E_{n\ell}$
		$[5f^2_{5/2}7s6d_{3/2}n\ell]$	$20543.-E_{n\ell}$
		$[5f^2_{5/2}6d^2_{3/2}n\ell]$	$20604.-E_{n\ell}$

Table 16. Molecular correlation diagram for N + O_2.

Reactants	Energy (eV)	States	Point Group
$N(^4S_u) + O_2(X^3\Sigma_g^-)$	1.401	$^{2,4,6}\Sigma^+$	$C_{\infty v}$
		$^{2,4,6}B_1$	C_{2v}
		$^{2,4,6}A'$	C_s
$N(^4S_u) + O_2(a^1\Delta_g)$	2.383	$^4\Delta$	$C_{\infty v}$
		$^4A_2, ^4B_1$	C_{2v}
		$^4A'', ^4A'$	C_s
$N(^4S_u) + O_2(b^1\Sigma_g^+)$	3.037	$^4\Sigma^-$	$C_{\infty v}$
		$^4A_2$	C_{2v}
		$^4A''$	C_s
$N(^2D_u) + O_2(X^3\Sigma_g^-)$	3.785	$^{2,4}\Sigma^+, ^{2,4}\Pi, ^{2,4}\Delta$	$C_{\infty v}$
		$^{2,4}B_1(2), ^{2,4}B_2, ^{2,4}A_2, ^{2,4}A_1$	C_{2v}
		$^{2,4}A''(2), ^{2,4}A'(3)$	C_s
$N(^2D_u) + O_2(a^1\Delta_g)$	4.766	$^2\Sigma^+, ^2\Sigma^-, ^2\Pi, ^2\Delta, ^2\Phi, ^2\Gamma$	$C_{\infty v}$
		$^2A_1(2), ^2A_2(3), ^2B_1(3), ^2B_2(2)$	C_{2v}
		$^2A'(5), ^2A''(5)$	C_s
$N(^2P_u) + O_2(X^3\Sigma_g^-)$	4.977	$^{2,4}\Sigma^-, ^{2,4}\Pi$	$C_{\infty v}$
		$^{2,4}A_1, ^{2,4}A_2, ^{2,4}B_2$	C_{2v}
		$^{2,4}A', ^{2,4}A''(2)$	C_s
$N(^2D_u) + O_2(b^1\Sigma_g^+)$	5.420	$^2\Sigma^-, ^2\Pi, ^2\Delta$	$C_{\infty v}$
		$^2A_1, ^2A_2(2), ^2B_1, ^2B_2$	C_{2v}
		$^2A'(2), ^2A''(3)$	C_s
$N(^4S_u) + O_2(c^1\Sigma_u^-)$	5.499	$^4\Sigma^+$	$C_{\infty v}$
		$^4A_1$	C_{2v}
		$^4A'$	C_s
$N(^4S_u) + O_2(A'^3\Delta_u)$	5.701	$^{2,4,6}\Delta$	$C_{\infty v}$
		$^{2,4,6}A_1, ^{2,4,6}B_2$	C_{2v}
		$^{2,4,6}A', ^{2,4,6}A''$	C_s

Table 16. Molecular correlation diagram for $N + O_2$ (Concluded).

Reactants	Energy (eV)	States	Point Group
$N(^4S_u) + O_2(A^3\Sigma_u^+)$	5.789	$2,4,6_{\Sigma^-}$	$C_{\infty v}$
		$2,4,6_{B_2}$	C_{2v}
		$2,4,6_{A''}$	C_s
$N(^2P_u) + O_2(a^1\Delta_g^+)$	5.958	$^2\Pi, \ ^2\Delta, \ ^2\Phi$	$C_{\infty v}$
		$^2A_1(2), \ ^2A_2, \ ^2B_1, \ ^2B_2(2)$	C_{2v}
		$^2A'(3), \ ^2A''(3)$	C_s
$N(^2P_u) + O_2(b^1\Sigma_g^-)$	6.612	$^2\Sigma^-, \ ^2\Pi$	$C_{\infty v}$
		$^2A_1, \ ^2B_1, \ ^2B_2$	C_{2v}
		$^2A'(2), \ ^2A''$	C_s

Products	Energy (eV)	States	Point Group
$NO(^2\Pi) + O(^3P_g)$	0	$^{2,4}\Sigma^+, \ ^{2,4}\Sigma^-, \ ^{2,4}\Pi, \ ^{2,4}\Delta$	$C_{\infty v}$
		$^{2,4}A'(3), \ ^{2,4}A''(3),$	C_s
$NO(^2\Pi) + O(^1D_g)$	1.967	$^2\Sigma^+, \ ^2\Sigma^-, \ ^2\Pi(2), \ ^2\Delta, \ ^2\Phi$	$C_{\infty v}$
		$^2A'(5), \ ^2A''(5)$	C_s
$NO(^2\Pi) + O(^1S_g)$	4.189	$^2\Pi$	$C_{\infty v}$
		$^2A', \ ^2A''$	C_s
$NO(a^4\Pi) + O(^3P_g)$	4.765	$^{2,4,6}\Sigma^+, \ ^{2,4,6}\Sigma^-, \ ^{2,4,6}\Pi, \ ^{2,4,6}\Delta$	$C_{\infty v}$
		$^{2,4,6}A'(3), \ ^{2,4,6}A''(3)$	C_s
$NO(A^2\Sigma^+) + O(^3P_g)$	5.450	$^{2,4}\Sigma^-, \ ^{2,4}\Pi$	$C_{\infty v}$
		$^{2,4}A', \ ^{2,4}A''(2)$	C_s
$NO(B^2\Pi) + O(^3P_g)$	5.693	$^{2,4}\Sigma^+, \ ^{2,4}\Sigma^-, \ ^{2,4}\Pi. \ ^{2,4}\Delta$	$C_{\infty v}$
		$^{2,4}A'(3), \ ^{2,4}A''(3)$	C_s
$NO(b^4\Sigma^-) + O(^3P_g)$	6.0344	$^{2,4,6}\Sigma^+, \ ^{2,4,6}\Pi$	$C_{\infty v}$
		$^{2,4,6}A'(2), \ ^{2,4,6}A''$	C_s

SECTION 6

LIST OF REFERENCES

1. Harang, O., "AlO Resonant Spectrum for Upper Atmosphere Temperature Determination," AFCRL-66-314, Environmental Research Paper, No. 192, 1966.

2. Churchill, D. R. and R. E. Meyerott, "Spectral Absorption in Heated Air," Journal of Quantitative Spectroscopy and Radiative Transfer, 5, p. 69, 1965.

3. The Airglow and the Aurorae, edited by E. B. Armstrong and A. Dalgarno. Pergamon Press, New York, 1955.

4. Armstrong, B. H., R. R. Johnston and P. S. Kelly,"The Atomic Line Contribution to the Radiation Absorption Coefficient of Air," Journal of Quantitative Spectroscopy and Radiative Transfer, 5, p. 55, 1965.

5. Johnston, R. R., B. H. Armstrong and O. R. Platas, "The Photoionization Contribution to the Radiation Absorption Coefficient of Air," Journal of Quantitative Spectroscopy and Radiative Transfer, 5, p. 49, 1965.

6. Michels, H. H. and F. E. Harris,"Valence Configuration Interaction Calculations for Atomic Scattering," International Journal of Quantum Chemistry, IIS, p. 21, 1968.

7. Harris, F. E. and H. H. Michels, "Open-Shell Valence Configuration – Interaction Studies of Diatomic and Polyatomic Molecules," International Journal of Quantum Chemistry, IS, p. 329, 1967.

8. Michels, H. H., "Molecular Orbital Studies of the Ground and Low-Lying Excited States of the HeH$^+$ Molecular Ion," Journal of Chemical Physics, 44, p. 3834, 1966.

9. Michels, H. H., "Ab Initio Calculation of the $B^2\Sigma^+ - X^2\Sigma^+$ Oscillator Strengths in AlO," Journal of Chemical Physics, 56, p. 665, 1971.

10. Michels, H. H., "Calculation of Electronic Wavefunctions," Final Report for AFOSR Contract F44620-74-C-0083, August 1975.

11. Michels, H. H., "Calculation of Potential Energy Curves for Metal Oxides and Halides," Final Report for AFOSR, Contract F44620-73-C-0077, May 1977.

12. Michels, H. H., "Theoretical Determination of Metal Oxide f-Numbers," Final Report for AFWL, Contract F29601-71-C-0119, Report AFWL-TR-74-239, May 1975.

13. Schaefer, F. E. and F. E. Harris, "Ab Initio Calculations of 62 Low-Lying States of the O_2 Molecule," Journal of Chemical Physics, 48, p. 4946, 1968.

14. Michels, H. H. and F. E. Harris, "Predissociation Effects in the $A^2\Sigma^+$ State of the OH Radical," Chemical Physics Letters, 3, p. 441, 1969.

15. Harris, F. E., "Open-Shell Orthogonal Molecular Orbital Theory," Journal of Chemical Physics, 46, p. 2769, 1967.

16. Roothan, C. C. J. and P. S. Bagus, "Atomic Self-Consistent Field Calculations by the Expansion Method," Methods in Computational Physics. Edited by B. Alder, 2, p. 47, 1963.

17. Givens, W., "Eigenvalue-Eigenvector Techniques," Oak Ridge Report Number ORNL 1574 (Physics).

18. Shavitt, I., C. F. Bender, A. Pipano, and R. P. Hosteny, "The Iterative Calculation of Several of the Lowest or Highest Eigenvalues and Corresponding Eigenvectors of Very Large Symmetry Matrices," Journal of Computational Physics, 11, p. 90, 1973.

19. Raffenetti, R. C., "A Simultaneous Coordinate Relaxation Algorithm for Large, Sparse Matrix Eigenvalue Problems," Journal of Computational Physics, 32, p. 403, 1979.

20. Harris, F. E. and H. H. Michels, "The Evaluation of Molecular Integrals for Slater-Type Orbitals," Advances in Chemical Physics, 13, p. 205, 1967.

21. Hehre, W. J., L. Radom, P. von R. Schleyer and J. A. Pople, Ab initio Molecular Orbital Theory, Wiley - Interscience, New York, 1986.

22. Dupuis, M., D. Spangler and J. J. Wendoloski, NRCC Software Catalog, Vol. 1, Program No. QG01 (GAMESS), 1980.

23. Davidson, E. R., "Natural Expansion of Exact Wavefunctions, III. The Helium Atom Ground State," _Journal of Chemical Physics_, 39, p. 875, 1963.

24. Wahl, A. C., P. J. Bertoncini, G. Das and T. L. Gilbert, "Recent Progress Beyond the Hartree-Fock Method for Diatomic Molecules, The Method of Optimized Valence Configurations," _International Journal of Quantum Chemistry_, IS, p. 123, 1967.

25. Ruedenberg, K., L. M. Cheung and S. T. Elbert, "MCSCF Optimization Through Combined Use of Natural Orbitals and the Brillouin-Levy-Berthier Theorem," _International Journal of Quantum Chemistry_, 16, p. 1069, 1979.

26. Slater, J. C., _Advances in Quantum Chemistry_, 6, p. 1, 1972.

27. Löwdin, P. O., "Quantum Theory of Many-Particle Systems. I. Physical Interpretations by Means of Density Matrices, Natural Spin-Orbitals, and Convergence Problems in the Method of Configurational Interaction," _Physical Review_, 97, p. 1474, 1955.

28. Kohn, W. and L. Sham, "Self-Consistent Equations Including Exchange and Correlation Effects," _Physical Review_, 140A, p. 1133, 1965.

29. Slater, J. C., "A Simplification of the Hartree-Fock Method," _Physical Review_, 81, p. 385, 1951.

30. Schwarz, K.: "Optimization of the Statistical Exchange Parameters α for the Free Atoms H Through Nb," _Physical Review_, B5, p. 2466, 1972.

31. Beebe, N. H. F., "On the Transition State in the X_α Method," _Chemical Physics Letters_, 19, p. 290, 1973.

32. Schwarz, K. and J. W. D. Connolly, "Approximate Numerical Hartree-Fock Method for Molecular Calculations," _Journal of Chemical Physics_, 55, p. 4710, 1971.

33. Connolly, J. W. D: unpublished results.

34. Slater, J. C., "Hellmann-Feynman and Virial Theorems in the X_α Method," _Journal of Chemical Physics_, 57, p. 2389, 1972.

35. Michels, H. H., R. H. Hobbs and J. C. Connolly, "Optimized SCF-X_α Procedures for Heterpolar Molecules," *Journal of Chemical Physics* (to be published).

36. Rosch, Notker and Keith H. Johnson, "On the Use of Overlapping Spheres in the SCF-X_α Scattered-Wave Method," *Chemical Physics Letters*, 23, p. 149, 1973.

37. Heitler, W., *The Quantum Theory of Radiation*. 3rd Edition, Oxford University Press, 1953.

38. Nicholls, R. W. and A. L. Stewart, *Allowed Transitions. Atomic and Molecular Processes*, D. R. Bates, Editor. Academic Press, 1962.

39. Penner, S. S., *Quantitative Molecular Spectroscopy and Gas Emissivities*, Addison-Wesley Publishing Company, Inc., 1959.

40. Dennison, D. M., "The Rotation of Molecules," *Physical Review*, 28, p. 318, 1926.

41. Kronig, R. and I. Rabi, "The Symmetrical Top in the Undulatory Mechanics," *Physical Review*, 29, p. 262, 1927.

42. Rademacher, H. and F. Reiche, "Die Quantelung des symmetrischen Kreisels nach Schrödingers Undulationsmechanik," *Zeitschrift fur Physik*, 41, p. 453, 1927.

43. Hönl, H. and F. London, "Intensities of Band Spectrum Lines," *Zeitschrift fur Physik*, 33, p. 803, 1925.

44. Herzberg, G., *Spectra of Diatomic Molecules*. 2nd Edition, Van Nostrand, 1950.

45. Fraser, P. A., "A Method of Determining the Electronic Transition Moment for Diatomic Molecules," *Canadian Journal of Physics*, 32, p. 515, 1954.

46. Breit, G., "The Effect of Retardation on the Interaction of Two Electrons." *Physical Review*, 34, p. 553, 1929; "The Fine Structure of He as a Test of the Spin Interactions of Two Electrons," 36, p. 383, 1930; "Dirac's Equation and the Spin-Spin Interactions of Two Electrons," 39, p. 616, 1932.

47. Bethe, H. A. and E. E. Salpeter, Quantum Mechanics of One- and Two-Electron Atoms. Academic Press, N. Y., 1957.

48. Hirschfelder, J. O., C. F. Curtiss and R. B. Bird, Molecular Theory of Gases and Liquids. John Wiley, N. Y., 1964.

49. Itoh, T., "Derivation of Nonrelativistic Hamiltonian for Electrons from Quantum Electrodynamics," Reviews of Modern Physics, 37, p. 159, 1965.

50. Kolos, W. and L. Wolniewicz, "Accurate Adiabatic Treatment of the Ground State of the Hydrogen Molecule," Journal of Chemical Physics, 41, p. 3663, 1964; "Accurate Computation of Vibronic Energies and Some Expectation Values for H_2, D_2, and T_2," 41, p. 3674, 1964; "Potential-Energy Curve for the $B^1\Sigma_u^+$ State of the Hydrogen Molecule," 45, p. 509, 1966.

51. Liberman, D., J. T. Waber, D. T. Cromer, "Self-Consistent Field Dirac-Slater Wave Functions for Atoms and Ions. I. Comparison with Previous Calculations," Physical Review, A137, p. 27, 1965.

52. Mann, J. B. and J. T. Waber, "SCF Relativistic Hartree-Fock Calculations on the Superheavy Elements 118-131," Journal of Chemical Physics, 53, p. 2397, 1970.

53. Grant, I. P.: "Relativistic Calculation of Atomic Structures," Advances in Physics, 19, p. 747, 1970.

54. Cowan, R. D.: "Atomic Self-Consistent-Field Calculations Using Statistical Approximations for Exchange and Correlation," Physical Review, 163, p. 54, 1967.

55. Desclaux, J. P., D. F. Mayers, and F. O'Brien, " Relativistic Atomic Wave Functions," Journal of Physics B, 4, p. 631, 1971.

56. Cowan, R. D. and D. C. Griffin, "Approximate Relativistic Corrections to Atomic Radial Wave Functions," Journal of the Optical Society of America, 66. p. 1010, 1976.

57. Wood, J. H. and A. M. Boring: "Improved Pauli Hamiltonian for Local-Potential Problems," Physical Review B, 18, p. 2701, 1978.

58. Boring, A. M. and J. H. Wood, "Relativistic Calculations of the Electronic Structure of UF_6," _Journal of Chemical Physics_, 71, p. 32, 1979.

59. Wood, J. H., A. M. Boring and S. B. Woodruff, "Relativistic Electronic Structure of UO_2^{++}, UO_2^{+} and UO_2," _Journal of Chemical Physics_, 74, p. 5225, 1981.

60. Michels, H. H., R. H. Hobbs and J. W. D. Connolly, "Electronic Structure and Photoabsorption of the Hg_2^{+} Dimer Ion," _Chemical Physics Letters_, 68, p. 549, 1979.

61. Weeks, J. D., A. Hazi and S. A. Rice: _Advances in Chemical Physics_, 16, p. 283, 1969.

62. Bardsley, J. N.: _Case Studies in Atomic Physics_, 4, p. 299, 1974.

63. Phillips, J. C. and L. Kleinman, "New Method for Calculating Wave Functions in Crystals and Molecules," _Physical Review_, 116, p. 287, 1959.

64. Hazi, A. U. and S. A. Rice, "Pseudopotential Theory of Atomic and Molecular Rydberg States," _Journal of Chemical Physics_, 45, p. 3004, 1966.

65. Tully, J. C., "Many-Electron Pseudopotential Formalism for Atomic and Molecular Excited-State Calculations," _Physical Review_, 181, p. 7, 1969.

66. Melius, C. F., B. D. Olafson and W. A. Goddard III, "Fe and Ni _Ab Initio_ Effective Potentials for Use in Molecular Calculations," _Chemical Physics Letters_, 28, p. 457, 1974.

67. Szasz, L. and G. McGinn, "Atomic and Molecular Calculations With The Pseudopotential Method. II. Exact Pseudopotentials for Li, Na, K, Rb, Be^{+}, Mg^{+}, Ca^{+}, Al^{++}, Cu and Zn^{+}," _Journal of Chemical Physics_, 47, p. 3495, 1967; "Atomic and Molecular Calculations with the Pseudopotential Method III: The Theory of Li_2, Na_2, K_2, LiH, NaH and KH; Pseudopotential Theory of Atoms and Molecules. II. Hylleraas-Type Correlated Pair Functions for Atoms With Two Valence Electrons," 56, p. 1019, 1972.

68. Kahn, L. R., P. Baybutt and D.G. Truhlar, "Ab Initio Effective Core Potentials: Reduction of All-Electron Molecular Structure Calculations to Calculations Involving Only Valence Electrons," Journal of Chemical Physics, 65, p. 3826, 1976.

69. Lee, Y. S., W. C. Ermler and K. S. Pitzer, "Ab Initio Effective Core Potentials Including Relativistic Effects. I. Formalism and Applications to the Xe and Au Atoms," Journal of Chemical Physics, 67, p. 5861, 1977.

70. Courant, R. and D. Hilbert, Methods of Mathematical Physics, Interscience, N.Y., 1961.

71. Froese-Fischer, C., Comp. Phys. Comm. 1, p. 151, 1969.

72. Kahn, L. R., P. J. Hay and R. D. Cowan, "Relativistic Effects in Ab Initio Effective Core Potentials for Molecular Calculations. Applications to the Uranium Atom," Journal of Chemical Physics, 68, p. 2386, 1978.

73. Desclaux, J. P.: Atomic Data and Nuclear Tables, 12, p. 311, 1973.

74. Krauss, M. O.: private communication.

75. Michels, H. H. and R. H. Hobbs, "Theoretical Study of the Radiative and Kinetic Properties of Selected Metal Oxides and Air Molecules," Final Report for DNA Contract DNA001-82-C-0015, DNA-TR-82-159, July 1983.

76. Michels, H. H. and R. H. Hobbs, "Theoretical Study of the Radiative and Kinetic Properties of Selected Metal Oxides and Air Molecules," Final Report for DNA Contract DNA001-83-C-0044, DNA-TR-85-156, May 1985.

77. Hulburt, H. M. and J. O Hirschfelder, "Potential Energy Functions for Diatomic Molecules," Journal of Chemical Physics, 9, p. 61, 1941.

78. Krauss, M. O. and W. S. Stevens, "The Electronic Structure and Spectra of UO^+," Chemical Physics Letters, 99, p. 417, 1983.

79. Heaven, M. C., J. Nicolai, S. J. Riley and E. K. Parks, "Rotationally Resolved Electronic Spectra for Uranium Monoxide," Chemical Physics Letters, 119, p. 229, 1985.

80. Kaledin, L. A., A. N. Kulikov, A. I. Kobylyanskii, E. A. Shenyavskaya and L. V. Gurvich, "Relative Position of a Group of Low-Lying States for the UO Molecule," Zhurnal Fizicheskoi Khimii, 61, N5, p. 1374, 1987.

81. Dulick, M., Ph.D. Thesis, M.I.T., 1982.

82. McGlynn, S. P. and J. K. Smith, "Electronic Structure, Spectra, and Magnetic Properties of Actinyl Ions. II. Neptunyl and the Ground States of Other Actinyls," Journal of Molecular Spectroscopy, 6, p.188, 1961.

83. Gritzner, G. and J. Selbin, "Studies of Dioxouranium (v) in Dimethylsulphoxide," Journal of Inorganic Nuclear Chemistry, 30, p. 1799, 1968.

84. Private communication.

85. Badger, R. M., "The Relation Between the Internuclear Distances and the Force Constants of Molecules and Its Application to Polyatomic Molecules," 3, p. 710, 1935.

86, Donovan, R. J. and D. Husain, "Recent Advances in the Chemistry of Electronically Excited Atoms," Chemical Reviews, 70, p. 489, 1970.

87. Gilmore, F., "Recommended Revision of the NORSE Calculation of NO Chemiluminescence from $N(^2P) + O_2$," RDA Technical Note dated November 17, 1986.

88. Private communication, H. H. Michels.

89. Dulick, M., E. Murad and R. F. Barrow, "Thermochemical Properties of the Rare Earch Monoxides," Journal of Chemical Physics, 85, p. 385, 1986.

90. Michels, H. H., "Theoretical Research Investigation for Air Molecular Calculations," Final Report for AFGL Contract F19628-80-C-0209, AFGL-TR-81-0151, April, 1981.

DISTRIBUTION LIST

DEPARTMENT OF DEFENSE

ASSISTANT TO THE SECRETARY OF DEFENSE
ATOMIC ENERGY
    ATTN: EXECUTIVE ASSISTANT

DEFENSE INTELLIGENCE AGENCY
2 CYS ATTN: RTS-2B

DEFENSE NUCLEAR AGENCY
    ATTN: RAAE
    ATTN: A MARDIGUIAN
    ATTN: B PRASAD
    ATTN: K SCHWARTZ
    ATTN: L WITTWER
4 CYS ATTN: TITL

DEFENSE NUCLEAR AGENCY
    ATTN: TDNM-CF
    ATTN: TDTT W SUMMA
    ATTN: TDTT

DEFENSE TECHNICAL INFO CENTER
12CYS ATTN: DD

LAWRENCE LIVERMORE NATIONAL LAB
    ATTN: DNA-LL

UNDER SECRETARY OF DEFENSE
    ATTN: DEFENSIVE SYSTEMS
    ATTN: STRAT & THEATER NUC FOR G SEVIN

DEPARTMENT OF THE ARMY

U S ARMY FOREIGN SCI & TECH CTR
    ATTN: DRXST-SD
    ATTN: DRXST-SD-3

DEPARTMENT OF THE NAVY

NAVAL OCEAN SYSTEMS CENTER
    ATTN: CODE 9642

NAVAL POSTGRADUATE SCHOOL
    ATTN: LIBRARY
    ATTN: PROF M N MILNE

NAVAL RESEARCH LABORATORY
    ATTN: J BROWN
    ATTN: TECH LIB)
    ATTN: J JOHNSON
    ATTN: W ALI
    ATTN: S OSSAKOW
    ATTN: J DAVIS
    ATTN: D STROBEL
    ATTN: C JOHNSON
    ATTN: J DAVIS
    ATTN: P PALMADESSO

DEPARTMENT OF THE AIR FORCE

AIR FORCE GEOPHYSICS LABORATORY
    ATTN: J PAULSON
2 CYS ATTN: R MURPHY
    ATTN: H GARDINER

2 CYS ATTN: R SHARMA
    ATTN: C PHILBRICK

AIR FORCE OFFICE OF SCI RSCH
    ATTN: AFOSR/NC

AIR FORCE TECH APPLICATIONS CTR
    ATTN: CA/STINFO
    ATTN: TX

AIR FORCE WEAPONS LABORATORY
    ATTN: SUL

AIR UNIVERSITY LIBRARY
    ATTN: AUL-LSE

DEPARTMENT OF ENERGY

DEPARTMENT OF ENERGY
    ATTN: F SPENCER

EG&G, INC
    ATTN: C ANDELARIA

LAWRENCE LIVERMORE NATIONAL LAB
    ATTN: A GROSSMAN
    ATTN: D WUEBBLES
    ATTN: G HAUGAN
    ATTN: E WOODWARD
    ATTN: H KRUGER

LOS ALAMOS NATIONAL LABORATORY
    ATTN: O JUDD
    ATTN: D SAPPENFIELD
    ATTN: W HUGHES
    ATTN: J MALIK
    ATTN: G M SMITH
    ATTN: M PONGRATZ
    ATTN: M SANDFORD
    ATTN: W BARFIELD
    ATTN: J ZINN
    ATTN: REPORT LIBRARY
    ATTN: R JEFFRIES
    ATTN: REPORT LIBRARY
    ATTN: T BIENIEWSKI

SANDIA NATIONAL LABORATORIES
    ATTN: L ANDERSON
    ATTN: M KRAMM
    ATTN: T P WRIGHT
    ATTN: W D BROWN
    ATTN: TECH LIB 3141

OTHER GOVERNMENT

ALBANY METALLURGY RSCH CENTER
    ATTN: E ABSHIRE

BUREAU OF MINES
    ATTN: J MURPHY

CENTRAL INTELLIGENCE AGENCY
    ATTN: OSWR/NED
    ATTN: L BERG

NATL OCEANIC & ATMOSPHERIC ADMIN
  3 CYS ATTN: F FEHSENFELD

NATIONAL SCIENCE FOUNDATION
      ATTN: A GROBECKER
      ATTN: R MCNEAL

DEPARTMENT OF DEFENSE CONTRACTORS

AERODYNE RESEARCH, INC
      ATTN: C KOLB

AEROJET ELECTRO-SYSTEMS CO
      ATTN: J GRAHAM

AEROSPACE CORP
      ATTN: C RICE
      ATTN: G LIGHT
      ATTN: H WANG

BERKELEY RSCH ASSOCIATES, INC
      ATTN: J WORKMAN

BOSTON COLLEGE
      ATTN: W GRIEDER

EOS TECHNOLOGIES, INC
      ATTN: B GABBARD
      ATTN: W LELEVIER

HSS, INC
      ATTN: N SHULER

INSTITUTE FOR DEFENSE ANALYSES
      ATTN: E BAUER
      ATTN: H WOLFHARD

JAMIESON SCIENCE & ENGINEERING
      ATTN: J JAMIESON

KAMAN SCIENCES CORP
      ATTN: E CONRAD

KAMAN SCIENCES CORPORATION
      ATTN: DASIAC

KAMAN TEMPO
  5 CYS ATTN: DASIAC

LOCKHEED MISSILES & SPACE CO, INC
      ATTN: J HENLEY
      ATTN: J PEREZ
      ATTN: R SEARS

MISSION RESEARCH CORP
      ATTN: R ARMSTRONG

MISSION RESEARCH CORP
      ATTN: D ARCHER
      ATTN: D SOWLE
      ATTN: R HENDRICK
      ATTN: W WHITE

PACIFIC-SIERRA RESEARCH CORP
      ATTN: E FIELD JR
      ATTN: H BRODE, CHAIRMAN SAGE

PHOTOMETRICS, INC
      ATTN: I KOFSKY

PHYSICAL RESEARCH INC
      ATTN: P LUNN

PHYSICAL RESEARCH, INC
      ATTN: T STEPHENS

PHYSICAL RESEARCH, INC
      ATTN: J DEVORE

PHYSICAL SCIENCES, INC
      ATTN: G CALEDONIA

PITTSBURGH, UNIV OF THE COMMONWEALTH
      ATTN: M BIONDI

R & D ASSOCIATES
      ATTN: F GILMORE

SCIENCE APPLICATIONS INTL CORP
      ATTN: D HAMLIN
      ATTN: D SACHS

SRI INTERNATIONAL
      ATTN: W CHESNUT

TOYON RESEARCH CORP
      ATTN: J ISE

UNITED TECH RSCH CENTER
  2 CYS ATTN: H MICHELS

VISIDYNE, INC
  2 CYS ATTN: J CARPENTER